IMPURITIES IN SOME WIDE-GAP SEMICONDUCTORS

Christer Ovrén

DEPARTMENT
OF
SOLID STATE PHYSICS

INSTITUTIONEN FÖR FASTA TILLSTÅNDETS FYSIK
LUNDS TEKNISKA HÖGSKOLA-LUNDS UNIVERSITET
LUND-SWEDEN

1978

IMPURITIES IN

SOME WIDE-GAP SEMICONDUCTORS

av

Christer Ovrén
Civ ing, Klm

AKADEMISK AVHANDLING

SOM FÖR AVLÄGGANDE AV TEKNISK DOKTORSEXAMEN
VID TEKNISKA FAKULTETEN VID UNIVERSITETET
I LUND KOMMER ATT OFFENTLIGEN FÖRSVARAS I
FYSISKA INSTITUTIONENS FÖRELÄSNINGSSAL B
FREDAGEN DEN 31 MARS 1978, KL 10.15

IMPURITIES IN

SOME WIDE-GAP SEMICONDUCTORS

by

Christer Ovrén

UNIV.
LEIDEN
BIBL.

IMPURITIES IN SOME WIDE-GAP SEMICONDUCTORS

by

Christer Ovrén

Department of Solid State Physics, Lund Institute of Technology

Box 725, S-220 07 Lund 7, Sweden

Introduction

This thesis is a study of how the optical and electrical properties of semiconductors are changed due to the presence of defects, either foreign atoms or native defects, in the material. The main part of the work has been carried out on the II - VI compound zinc-selenide, but also the III - V semiconductor gallium-phosphide has been the subject of investigations. A feature common to both these semiconductors is their large band-gaps (E_g=2.70 eV for ZnSe[1] and E_g=2.26 eV for GaP[2] at room temperature), which makes them not only interesting from the purely physical points of view, but also as possible materials in applications such as light-emitting devices. The results obtained are presented in the following papers:

I Photoionization selection rules for deep oxygen states in GaP.
Proceedings of the 12:th International Conference on the Physics of Semiconductors.
(Stuttgart 1974).
(together with H G Grimmeiss, L-Å Ledebo, Lund and T N Morgan IBM, USA)

II Investigations of Mn-doped ZnSe by photocapacitance and photocurrent techniques.
Journal of Applied Physics 47, 1103 (1976)
(together with H G Grimmeiss, Lund and J W Allen, St Andrews, Scotland)

III Identification of deep centers in ZnSe.
Journal of Applied Pysics 48, 5122 (1977)
(together with H G Grimmeiss, Lund and W Ludwig, R Mach, Berlin, East-Germany)

IV Optical and electrical properties of the red copper center in ZnSe.
Manuscript.

Before summarizing the results of the papers, some general problems connected with impurities in semiconductors will be discussed and concepts used in the papers introduced. A short discussion of the methods employed, is given and some applications in which impurities are of importance are mentioned.

Shallow and deep level impurities.

The optical and electrical properties of semiconductors can vary considerably due to the presence of small amounts of impurities which can be introduced into the crystal, e g by the addition of foreign atoms when growing the material. This is one of the main reasons for the considerable technological importance of semiconductors. As typical examples, it is well-known that the electrical resistivity of silicon can be changed by several orders of magnitude and made either n-type or p-type by the addition of about 1 ppm of arsenic or boron and that, by doping with different impurities, the spectral response of photosensitive resistors can be altered to fit specific applications.

Starting from the properties of the perfect crystal, the impurity problem can be formulated in the following equations[3]:

The equation

$$H^0 \psi^0_{n,\vec{k}} = \left(-\frac{\hbar^2}{2m}\nabla^2 + V^0\right) \psi^0_{n,\vec{k}} = E^0_{n,\vec{k}}\, \psi^0_{n,\vec{k}} \qquad (1)$$

is the eigenvalue problem for the perfect crystal. Here, V^o is the periodic potential, $\Psi^o_{n,\vec{k}}$ Bloch states and $E^o_{n,\vec{k}}$ the bandstructure for the perfect crystal. The corresponding equation for a crystal containing impurities is

$$H\Psi = (-\frac{\hbar^2}{2m}\nabla^2 + V)\,\Psi = E\Psi \tag{2}$$

By the expansion

$$\Psi(\vec{r}) = \sum_{n,\vec{k}} A_{n,\vec{k}}\,\Psi^o_{n,\vec{k}}(\vec{r}) \tag{3}$$

the following set of equations is obtained

$$E^o_{n,\vec{k}}\,A_{n,\vec{k}} + \sum_{n',\vec{k}'} \langle \Psi^o_{n,\vec{k}} \,|U|\, \Psi^o_{n',\vec{k}'} \rangle\, A_{n',\vec{k}'} = E\,A_{n,\vec{k}} \tag{4}$$

where $U(\vec{r}) = V(\vec{r}) - V^o(\vec{r})$, the impurity potential, is of fundamental importance for determining the influence of the impurity on the properties of the material.

If an atom of the host lattice is substituted by an atom belonging to one of the nearest groups in the periodic table, e g, phosphorous on a substitutional site in silicon, the potential U(r) binding the extra electron at the phosphorous atom, can be approximated by a hydrogenic-like potential,

$$U(\vec{r}) = -\frac{e^2}{4\pi\varepsilon\varepsilon_o r}\,. \tag{5}$$

This potential gives rise to an energy level in the bandgap below the conduction band edge for the ground impurity state and, in addition, a ladder of excited states. In most semiconductors, the energy distance between the band edge and the ground state level is small for impurities which can be described using equation (5), typically less than 0.1 eV. Such impurities, called shallow donors or shallow acceptors (depending on whether the substituting atom has one electron more or one electron less than the replaced host atom), are well understood within the so-called "effective-mass theory"[4,5]. This theory

has been improved in recent years taking into better account the actual bandstructure and the screening properties of the semiconductor and the individual nature of the impurity atom[3,6-8]. Good quantitative agreement between calculated energy levels and experimental data has been obtained for several acceptor and donor states in silicon, germanium and the III-V compounds.

Because of the small ground-state energy, the extra carriers introduced by these impurities (electrons in the case of donors and holes in the case of acceptors) are released already at temperatures well below room temperature and appear as mobile carriers in the conduction or valence band. Doping with shallow impurities is generally used to influence the conductivity of semiconductors.

Impurities other than those discussed above will in general create energy levels farther away from the band edges and are therefore often called deep-level impurities[9,10]. The impurities studied in this thesis belong to this group. The effective mass theory is not in general applicable to these states. Several calculations[11-14] of the energy levels introduced by deep impurities have been made, both along the lines of equation (4) and using other methods, such as e g, molecular-orbital techniques in which the crystal is represented by the impurity atom in a cluster of finite size. In the crystal-field theory[15], which has been used to explain some of the properties of transition metal and rare earth impurities, the electronic states of the free ions are modified by the electric field in the crystal. The understanding of deep impurity states is, however, relatively modest compared to that of centers, which can be treated within the effective-mass theory.

Deep impurities often create efficient channels for the recombination of electrons with holes[10] and are thus very important for the determination of carrier lifetimes, even when the concentration of these impurities in the material is small.

A review of theoretical treatments of impurity levels in semiconductors is given in reference 16.

Excitation and recombination processes.

The influence of an impurity on the optical and electrical properties of a semiconductor can be described by introducing emission rates and capture constants for excitation and recombination processes for carriers at the impurity[17]. These concepts are defined in figure 1, where an impurity with two charge states is considered.

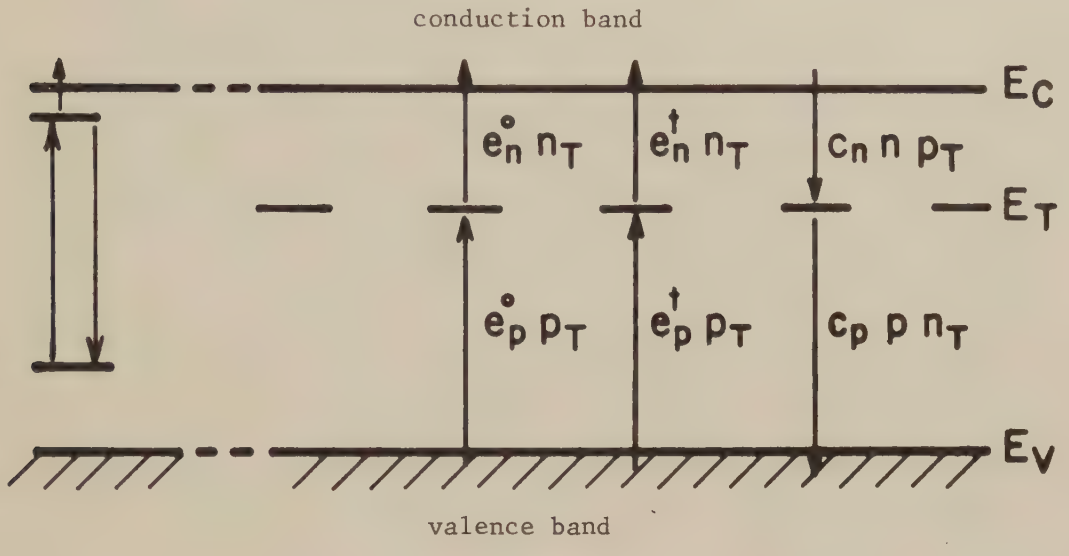

Figure 1

e_n^o and e_n^t are emission rates for the excitation of electrons from the impurity level to the conduction band, e_n^o denotes optical excitation and e_n^t thermal excitation processes. e_p^o and e_p^t are the corresponding quantities for the excitation of electrons from the valence band into the impurity level. The unit for emission rates is seconds^{-1}. c_n and c_p are capture constants, usually expressed in the unit cm^3 sec^{-1}. These constants describe the capture of carriers from band states into the bound impurity state. The capture constants are often written as the sum of capture constants for different recombination processes, e g, as the sum of radiative and non-radiative recombination

$$c_n = c_n^o + c_n^t \qquad (6)$$

n_T denotes the number of impurity states per unit volume which are occupied with electrons and p_T is the number of unoccupied states.

If the impurity has only two charged states, then

$$n_T + p_T = N_{TT} \tag{7}$$

where N_{TT} is the concentration of impurity states. n and p are the concentrations of electrons in the conduction band and of holes in the valence band respectively. N_{TT}, n_T, p_T, n, p all have the unit of cm^{-3}.

The following rate equations can be used to describe transitions between the impurity level and the bands:

$$\frac{dn}{dt} = e_n^o \cdot n_T + e_n^t \cdot n_T - c_n \cdot n \cdot p_T \tag{8}$$

$$\frac{dp}{dt} = e_p^o \cdot p_T + e_p^t \cdot p_T - c_p \cdot p \cdot n_T \tag{9}$$

$$\frac{dn_T}{dt} = (e_p^o + e_p^t) p_T - (e_n^o + e_n^t) n_T + c_n \cdot n \cdot p_T - c_p \cdot p \cdot n_T \tag{10}$$

By solving these equations, it is possible to calculate different properties of the material, which are determined by the impurity, e g, the photoconductivity of the material under a certain illumination.

Other important processes which are indicated in figure 1 are transitions between two bound states, e g, the ground state and an excited state of an impurity. Such excitations can be followed either by recombination back into the ground state or by a subsequent excitation (e g, by optical, thermal or field-assisted processes) releasing the carrier into a band.

Besides appearing in the kinetic equations for excitation and recombination processes, the parameters defined in figure 1 are important since they are easily converted into more basic physical parameters. From optical emission rates, optical cross sections can be calculated by division with the photon flux (L) of the incident light.

We have

$$\sigma_n^o = \frac{e_n^o}{L} \tag{11}$$

for optical excitations from the impurity level into the conduction band. Optical cross sections are calculated in the dipole approximation using Fermis Golden Rule

$$\sigma^o(h\nu) \sim \frac{1}{h\nu} |< \Psi_i|p|\ \Psi_f >|^2\ \rho(h\nu - E_I). \tag{12}$$

$h\nu$ is the photon energy. $\rho(h\nu-E_I)$ is the density of states in the band for the case when the initial electronic state is the impurity state at an energy E_I from the band. Ψ_f represents a state in the band. Optical cross sections are usually measured as a function of the photon energy of the incident light and the threshold energy for the excitation process is used to estimate the position of the impurity level in the bandgap. The density of final states, $\rho(E)$, is a property of the undoped crystal. If Ψ_f is taken as Bloch states, optical cross sections can be calculated using equation 12 and by comparing with experimental data a possibility of testing different impurity wavefunctions is given. From such calculations, it is also possible to obtain a more exact value for the energy position of the impurity level. Many calculations of optical cross sections have been made[18-30]. Two common approximations which are made are that the band states are taken to be plane waves and that the bands are considered as parabolic. Furthermore, evaluations of optical cross sections are usually carried out using general expressions for Ψ_i, taken as the ground state wave-function either for a hydrogenic potential[18] in the case of shallow levels or as the wave-function for a delta-function potential[19] in the case of deep levels. From measured spectra, information about the bandstructure[29] or about impurity wave-functions[30] has also been extracted. Recently, attempts have been made[20] to include the actual band structure of silicon in the calculation of optical cross sections for various impurities in this material using a density of states computed with the $\vec{k} \cdot \vec{p}$-method.

A further problem when interpreting impurity spectra is that of electron-phonon interactions in the optical transitions. Because the wave-function for the carrier in the bound impurity state is far more localized than the wave-functions for the band states, a change of the electronic state can give rise to changes in the vibrational properties of the lattice. A simple model for treating these problems is the so-called "configuration coordinate model"[31-35]. This was originally developed to treat transitions between discrete energy states and has been applied to luminescence and absorption spectra in II-VI and III-V compounds. It has also been extended to the case where one state represents a state in a band[27,36-39]. Using the adiabatic approximation[40], which rests essentially upon the fact that the mass of the nucleus is large in comparison with the electron mass, the wavefunction can be written as the product

$$\Phi(\vec{r},\vec{R}) = \Psi(\vec{r},\vec{R})\ \chi_e(\vec{R}) \tag{13}$$

where $\chi_e(\vec{R})$, the vibrational wave-function, is a function only of the lattice coordinates $\vec{R}$, but depends on the electronic state e. $\Psi(\vec{r},\vec{R})$ is the electronic wave-function which depends on the electron coordinates $\vec{r}$ and on the lattice coordinates $\vec{R}$. The matrix element which governs optical transitions

$$< \Phi_i(\vec{r},\vec{R})|\tilde{H}_{rad}|\Phi_f(\vec{r},\vec{R})> \tag{14}$$

can then be separated into two parts and written[40] as

$$<\Psi_i(\vec{r})|\tilde{H}_{rad}|\Psi_f(\vec{r})> <\chi_{ie}(\vec{R})|\chi_{fe}(\vec{R})> \tag{15}$$

in the Condon approximation, in which the first matrix element is evaluated for a constant $\vec{R}$ during the excitation. The first matrix element describes, as in (12), the optical transitions between the two electronic states and the second matrix element depends on the coupling between the electronic states and the lattice vibrational modes.

Capture cross sections are usually derived[41] from capture constants by the relation

$$\sigma_n = \frac{c_n}{v_{th}} \tag{15}$$

where v_{th} is the mean thermal velocity for the electrons. Recombination occurs through a variety of mechanisms, both by radiative and by non-radiative processes. A review of theoretical treatments is given in reference 42. One problem is to account theoretically for the various values and the temperature dependence of capture cross sections reported for deep impurities. Recently however, the capture of electrons and holes at several deep states in GaAs and in GaP has been attributed to recombination by multi-phonon emission[43].

Some of the parameters for the impurity defined in figure 1 can be related to each other by general expressions. By using the principle of detailed balance, the following relation between the capture cross section and the thermal emission rate can be obtained

$$e_n^t = g \cdot \sigma_n^t \cdot v_{th} \cdot N_c \cdot e^{-\frac{(E_c - E_T)}{kT}} \tag{16}$$

g is a degeneracy factor.

This relation is used to calculate the thermal ionization energy from measurements of thermal emission rates and capture cross sections as a function of temperature. The same principle can be applied to give a relation[44] between the optical cross sections for absorption processes and the radiative capture cross sections for recombination processes.

Measurement techniques.

The methods for measuring emission rates and capture cross section used in this thesis can be divided into two classes, one in which bulk material is used and one using junctions. In the latter, the

space charge region of a pn-junction or a Schottky diode is used for the investigations[10].

In photoluminescence measurements, the radiative recombination is analysed. The luminescence spectra give information about radiative capture processes and in addition both the excitation spectra and the optical quenching of the luminescence, can be used to yield optical cross sections for absorption processes. Luminescence investigations require no device fabrication, only a piece of bulk material being needed, but they can be used only if the recombination of the excited carriers has a radiative part. Optical cross sections are also studied in bulk material with photoconductivity measurements, in which the change in conductivity of a homogeneous semiconductor due to illumination is studied. This method requires the preparation of ohmic contacts on the sample. One disadvantage of these two techniques is that the measured signal often depends on both the excitation and the recombination parameters of the impurity.

In junction techniques, the current or the capacitance of the device is monitored. The values and the time-dependence of these signals are studied when the illumination, the bias or the temperature is varied.

With junction methods, only processes which take place at impurities located within the depletion region of the junction contribute to the measured signals, that is, give rise to reverse currents or cause capacitance changes. With the intensities normally used, it can be assumed that the free carrier concentration within the depletion region can be neglected. Thus, n=p=0 in equations 8-10 and together with equation 7 we obtain e g from equation 10,

$$\frac{dn_T}{dt} = (e_p^o + e_p^t)\cdot(N_{TT}-n_T) - (e_n^o + e_n^t)\cdot n_T \qquad (17)$$

showing that only excitation processes are determining the measured signals. Furthermore, the excitation processes can be separated from each other, by making measurements at low enough temperatures and in the dark.

Junctions can also be used in the study of recombination processes. This can be done by reducing the depletion region width with short voltage pulses, during which recombination can take place. In darkness, at low temperatures, equation 10 then reduces to

$$\frac{dn_T}{dt} = c_n \cdot n \cdot p_T - c_p \cdot p \cdot n_T \qquad (18)$$

and can be used to determine the capture constants.

A further advantage of junction methods is that absolute values of excitation and recombination parameters are easily obtained. Emission rates are calculated directly as the reciprocal of the time constant in transient measurements and the determination of capture cross sections requires, in addition, only a knowledge of the free carrier concentration, which can be measured with standard methods. Junction methods also allow the determination of the concentration of impurity states.

A problem connected with junction techniques is that the performance of the devices, in terms of leakage currents and series resistance, is critical. This is the case because, with realistic doping concentrations and junction areas, relatively small currents (typically $< 10^{-12}$ A) and capacitance changes (typically < 1%) have to be measured. These disadvantages can be avoided with the modified photocapacitance method used in paper IV. Another problem is that the electric field in the junction can affect the quantities studied. It is therefore valuable to compare results obtained from junctions with results obtained from bulk material.

A review covering different measuring techniques is given in reference 10.

Identification of impurity states.

With the measurement techniques discussed above, transitions between impurity energy levels and bands or between impurity levels are studied. From such measurements, conclusions about the energy position of the involved levels and about the properties of the impurity states creating these levels are drawn. The origin of such impurity or

defects states can be, e g a substitutional or an interstitial foreign atom, a vacancy, some form of dislocation or a surface state. In addition, two or more of these defects can interact, forming complexes.

The diffusion coefficient and the maximum solubility of different impurity atoms vary considerably[41], the solubility of deeper impurities tending to be lower[9]. It has also been shown that temperature cycles, to which the samples might be subjected in the doping process, sometimes introduce impurity states[45]. It is therefore not sufficient to identify an impurity state with a chemical element by correlating an "impurity signal" with the preparation procedure only, but measurements which give the concentration of that element in the sample have also to be made. The small concentrations involved require a high sensitivity for any method used for such "chemical" analysis. The following methods have been used in this thesis:

Atomic absorption[46]- In this method, the sample is "atomized" and characteristic absorption lines for different elements are measured.

Radiotracer technique - The sample is in this method doped with radioactive impurity atoms and the activity from the sample is monitored. These two methods give the total concentration of the chemical element in the sample.

EPR-electron paramagnetic resonance[47]- In these investigations, the structure of the measured spectra is used to obtain the symmetry around the impurity and can give information about the position of the impurity in the lattice. The magnitude of the signal can be used to calculate the concentration of the impurities contributing to the signal. By optical excitation, this method can be used also to measure optical emission rates.

Measurements of properties of the impurity in samples having different concentration and different chemical identity of the shallow doping and different vacancy concentration can yield information about the formation of complexes.

A positive identification of most of the deep impurities hitherto studied has not yet been possible, although such an identification has to be the basis of any theoretical treatment of the impurity problem taking into account the individual nature of the impurity. Also, to

improve those properties of semiconductor devices which are determined by impurity states, the origin of these states has to be known.

Importance in applications.

Doping with shallow impurities is used to fabricate a wide variety of semiconductor devices, the best-known being diodes, transistors and integrated circuits. The performance of many of these devices can be considerably improved by a precise control of the impurities giving rise to deep states. As examples, it can be mentioned that the fabrication of high-power rectifiers and thyristors requires silicon in which the impurity concentration is extremely low and that, in the manufacture of fast switching-diodes or transistors of silicon, doping with gold, thus creating deep impurity levels, which act as recombination centers, is often used. The presence of unwanted impurities in light-emitting devices of, e g GaP, can introduce non-radiative recombination channels, thereby reducing their efficiency.

One of the reasons for the current interest in ZnSe is that this material offers a possibility of producing cheap light-emitting devices, emitting light of any desired colour in the visible region. ZnSe has good luminescence properties and various emissions can be obtained by doping with different impurities, such as Cu[48] and Mn[49]. One major problem to be solved is that of excitation. In order to be applicable commercially, a low-voltage dc excitation method would be advantageous. With III-V compounds, this is often realized by minority carrier injection obtained with pn-junctions working in the forward direction. Light-emitting devices of ZnSe, interpreted as pn-junctions working according to this principle, have been reported. These devices have been fabricated both by the diffusion[50,51] of Ga, In and Tl and by ion-implantation[52,53] of e g P and N. It seems however, to be very difficult to produce ZnSe as a p-type material of sufficiently high conductivity and therefore attempts have been made to solve the injection problems by other means. One way to do this[54,55] is to use Schottky diodes made with n-type material. If the conductivity of the semiconductor is high, the depletion region of such a device will be narrow and electrons can tunnel through the barrier even at low reverse voltages, thus giving rise to a reverse current. With an electric field in the junction, which is high enough, the electrons

can gain sufficient energy to ionize impurities present or the lattice by impact. If the recombination processes which take place are radiative, light is emitted. A method of injecting holes is to apply a forward voltage to a metal-insulator-semiconductor structure. In this way, blue emissions caused by recombination of excitons or by pair emissions have been obtained with ZnSe[1,56]. One problem with these MIS-structures is the fabrication of oxide layers which are thin enough and yet stable.

Summary of the papers.

The first of the papers in this thesis deals with gallium phosphide doped with oxygen. Oxygen is known to give rise to a deep donor state in this material, when incorporated substitutionally on phosphorous sites.Different properties of this center have been the subject of studies with photoluminescence techniques[57] and with current[58,59] and capacitance[38,60] methods using pn-junctions. These investigations place the ground state level for this state (the O_I-state) at about 0.9 eV below the conduction band. With junction methods[38,60], it has been shown that, in addition to this state, oxygen can bind a second electron (the O_{II}-state). The results for the O_{II}-state from these investigations[38,60] have been interpreted in a configuration coordinate model with very large relaxation effects. From the optical cross section spectra, a threshold energy of about 2.0 eV and a binding energy of 1.23 eV for the second electron related to the conduction band were calculated[38]. However, the same model applied to thermal emission rates gave 0.76 eV[38] or, from later investigations, 0.89 eV[43] for this energy separation. The photoconductivity properties of oxygen-doped gallium phosphide are investigated in paper I, for comparison with results obtained with bulk material. The method which is used enables one to obtain in a direct way from the measurements the spectral dependence of the optical cross section for the transitions involved. The presence of oxygen in the samples is confirmed using different techniques, such as photoluminescence. Assuming the O_{II}-state to have a p-like character, the optical cross section obtained from these investigations is interpreted as arising from excitations from this state into different parts of the conduction band. This interpretation places the O_{II}-state at about 0.65 eV below the conduction band.The differences between the results obtained with the two methods have been attributed[61] to effects of the electric field in the junction. Recent

photoluminescence excitation experiments[57] and a re-interpretation[62] of luminescence data obtained with oxygen-doped GaP suggest that the position of the O_{II}-level is at about 0.9 eV below the conduction band and that relatively small relaxation effects are involved.

Papers II, III and IV contain studies of zinc selenide. In paper II, junction techniques are applied to the study of impurity states in this material. Paper III deals with the question of the identity of the impurity states. In paper IV, the emission and capture parameters for an impurity state, which is found in paper III to be introduced by Cu-doping, are studied and the results are analysed within a model for the impurity system.

Because of the difficulties of preparing low-ohmic p-type ZnSe and thus pn-junctions of this material, investigations of impurities in this semiconductor using junction techniques must be carried out with Schottky diodes fabricated on n-type material. The investigations of Mn-doped ZnSe with photocapacitance and photocurrent techniques which are presented in paper II reveal an impurity level located in the lower half of the bandgap, with a threshold energy for optical excitations from the valence band into the impurity level at about 0.68 eV. In paper II, it is demonstrated how the optical cross sections (σ_n^o and σ_p^o) for this center can be investigated at different temperatures in the presence of other impurities in the sample. With the methods used, the contributions to the measured signals arising from impurities other than the one subject to investigation, can be eliminated and thus the parameters for the particular impurity of interest obtained. The concentration of impurity centers is also determined.

In paper II it is also shown that by using optical excitation, thermal emission rates for the impurity level studied, located in the lower half of the bandgap, can be measured with Schottky diodes on n-type material. Such impurity levels are commonly studied with n^+p-junctions or Schottky diodes on p-type material. To increase the sensitivity of the method in the temperature range where thermal emission rates are small, optical excitation is used also for monitoring the change of charge at the centers, which takes place due to the thermal excitation.

In paper III, the measurement techniques of paper II are used to identify impurity states in ZnSe. Using the property of selecting out the contributions to the signal from different impurities possessed by these methods, the presence of different impurity centers contributing to the photocurrent or photocapacitance signal is studied. Special interest is focused on the impurity state which was detected in paper II and the concentration of this impurity, as obtained from the junction measurements, is correlated with the other properties of the material, grown in different ways and with different concentrations of dopants.

Crystals prepared by two different growth methods are investigated and measurements are made with material which is either non-intentionally doped, Mn-doped or Cu-doped, the doping being carried out under different conditions. The presence of Mn and Cu in the material is established using a number of methods. From atomic-absorption measurements, the concentration of Mn- and Cu-atoms in the crystal is obtained. The incorporation of Mn on substitutional lattice sites is checked with EPR-measurements. Using radio-tracer techniques, it is also shown in paper III that the concentration of Cu in the crystals can be influenced by treatments in solutions of Zn, with and without the addition of Cu.

The luminescence properties of the samples were also investigated, revealing the presence of two emissions in photoluminescence, the so called "Cu-red" emission, obtained in previous studies[48,63] of Cu-doped material and the "self-activated" emission[48], which is believed to be due to a complex between a shallow donor and a vacancy. Using reverse-biased Schottky diodes fabricated on Mn-doped material, the spectrum attributed to Mn in earlier investigations[49,64] was obtained in electroluminescence.

From the investigations reported in paper III, an impurity level in the lower half of the bandgap was identified as being caused by Cu. It is also shown to be identical with the impurity level at about 0.68 eV above the valence band which had been previously detected in Mn-doped ZnSe during the work reported in paper II. By measuring the spectrum of optical quenching of the Cu-red emission in photoluminescence and comparing it with the optical cross section spectrum obtained from

photocapacitance, it is also concluded that this center is responsible for the Cu-red emission.

No impurity level introduced by the Mn-doping was detected with the junction techniques employed, although the concentration of Mn-atoms in the sample was measured to be as high as 10^{19} cm^{-3}. A further energy level in the lower half of the bandgap was found in the samples, independent of the doping. It is suggested that this level is connected with the self-activated luminescence in ZnSe.

The results from paper III also show the problem of Cu-contamination of ZnSe. With the growth methods used, Cu is introduced non-intentionally into the crystals and unless these are subjected to careful purification, e g by repeated aftertreatments in liquid Zn, Cu is not sufficiently removed from the material, but remains to contribute to measured signals. Thus, besides being detected in Cu-doped ZnSe, the Cu-red center was, as shown in paper III, also present in some of the undoped and Mn-doped samples, although in smaller concentrations.The Cu-red center has a threshold for optical excitations from the impurity level into the conduction band at about 2.1 eV at room temperature. Thresholds at about this energy have also been reported in earlier photocapacitance studies of Mn-doped ZnSe[65] and of Ni-doped ZnSe[66], presumably due to residual Cu-contamination.

In paper IV, the properties of the Cu-red center are studied. The knowledge of the influence of the preparation techniques on the concentration of this impurity state, which was gained in the work reported in paper III is used to prepare samples with optimal properties for investigating this impurity with junction techniques. Due to the good experimental conditions, the optical cross sections for this state are measured with higher accuracy than has been possible in earlier investigations and are found to be slightly temperature dependent. The temperature range for these measurements is also extended to lower temperatures, down to 40K, and the thermal emission rates remeasured with a better accuracy than before. Using a combination of optical excitation and pulsed capacitance techniques, the capture cross section σ_n for the capture of electrons from the conduction band into the Cu-red level, is measured in the temperature range 77-200K.

In order to compare results obtained with junction techniques with results obtained from measurements on bulk material, photoconductors of Cu-doped ZnSe were investigated. By studying the optical quenching of photoconductivity at different temperatures, it is shown in paper IV that the influence of the electric field in the junction on the optical spectra can be neglected.

The more accurate data for emission and capture processes are taken as the basis of an analysis of the impurity system. It is found that the general features of the temperature-dependence of the optical cross section spectra for absorption can be explained if electron-phonon interactions in transitions via the center are taken into account. This has been done using the configuration coordinate model, with a coupling constant and a phonon energy characterizing this interaction taken from the photoluminescence spectrum. The shape of the optical cross sections can be understood, if not only optical excitations from the impurity ground state into the band states are considered but also excitations to other discrete energy levels. The origin of these levels can not be established from these investigations, but it is suggested that one of them arises either from the crystal-field splitting of a Cu d-state or from a coulombic part in the potential binding the carrier.

Acknowledgements.

I wish to express my sincere thanks to professor Hermann Grimmeiss for his continuous support and interest in my work.

I would like to thank my co-authors for a fruitful and stimulating co-operation.

Special thanks are due to tekn dr Stellan Braun for his expert guidance during the introductory phase of these investigations.

The discussions with the Solid-State Group at the Theoretical Department are also greatly acknowledged.

Finally, I would like to thank all members of our Department for their support and for many stimulating discussions during the time this work was carried out.

References.

1. M.D.Ryall and J.W.Allen, J.Phys.Chem.Solids 34, 2137 (1973)
2. P.J.Dean and D.G.Thomas, Phys.Rev. 150, 690 (1966)
3. S.T.Pantelides, Festkörperprobleme XV, 149 (1975)
4. J.M.Luttinger and W.Kohn, Phys.Rev. 97, 869 (1955)
5. W.Kohn, Solid State Phys. 5, 257 (1957)
6. S.T.Pantelides and C.T.Sah, Phys.Rev. B 10, 621 (1974)
7. A.Baldereschi and N.O.Lipardi, Phys.Rev. B 9, 1525 (1974)
8. J.Bernholc and S.T.Pantelides, Phys.Rev. B 15, 4935 (1977)
9. H.J.Queisser, Festkörperprobleme XI, 45 (1971)
10. H.G.Grimmeiss, Ann.Rev.Mater.Sci. 7, 341 (1977)
11. R.P.Messmer and G.D.Watkins, Phys.Rev. B 7, 2568 (1973)
12. M.Jaros and S.F.Ross, J.Phys. C 6, 1753 (1973)
13. M.Jaros and S.Brand, Phys.Rev. B 14, 4494 (1976)
14. K.A.Kikoin and V.N.Fleurov, J.Phys. C 10, 4295 (1977)
15. J.S.Griffith, Theory of Transition-Metal Ions (Cambridge 1961)
16. F.Bassani,G.Iadonisi and B.Preziosi, Rep.Prog.Phys. 37, 1099 (1974)
17. W.Shockley and W.T.Read Jr, Phys.Rev. 87, 835 (1952)
18. W.W.Anderson, Solid-State Electron. 18, 235 (1975)
19. G.Lucovsky, Solid State Commun. 3, 299 (1965)
20. S.T.Pantelides and J.Bernholc, Inst.Phys.Conf.Ser. 31, 465 (1977)
21. D.M.Eagles, J.Phys.Chem.Solids 16, 76 (1960)
22. J.W.Allen, J.Phys. C 2, 1077 (1969)
23. H.B.Bebb, Phys.Rev. 185, 1116 (1969)
24. H.B.Bebb and R.A.Chapman, J.Phys.Chem.Solids 28, 2087 (1967)
25. H.Kukimoto,S.Shinoya,T.Koda and R.Hioki, J.Phys.Chem.Solids 29, 935 (1968)
26. T.H.Ning and C.T.Sah, Phys.Rev. B 14, 2528 (1976)
27. M.Jaros, Phys.Rev. B 16, 3694 (1977)
28. Y.S.Matronitskii,Y.A.Pozneritsa and A.G.Cheban, Sov.Phys.Semicond. 7, 788 (1973)
29. H.G.Grimmeiss and L-A.Ledebo, J.Phys. C 8, 2615 (1975)
30. E.F.Rynne,J.R.Cox,J.B.McGuire and J.S.Blakemore, Phys.Rev.Lett. 36, 155 (1976)
31. K.Huang and A.Rhys, Proc.Roy.Soc. A204, 406 (1950)
32. M.Lax, J.Chem.Phys. 20, 1752 (1952)
33. D.L.Dexter, Solid State Phys. 6, 353 (1958)

34. T.H.Keil, Phys.Rev. 140, A601 (1965)
35. C.S.Kelley, Phys.Rev. B 6, 4112 (1972)
36. J.M.Dishman and M.DiDomenico Jr, Phys.Rev. B 4, 2621 (1971)
37. A.A.Kopylov and A.N.Pikhtin, Sov.Phys.Solid State 16, 1200 (1974)
38. H.Kukimoto,C.H.Henry and F.R.Merrit, Phys.Rev. B 7, 2486 (1973)
39. B.Monemar and L.Samuelson, J.Luminescence 12/13, 507 (1976)
40. K.K.Rebane, Impurity Spectra of Solids (New York 1970)
41. A.G.Milnes, Deep Impurities in Semiconductors (New York 1973)
42. A.Haug, Festkörperprobleme XII, 411 (1972)
43. C.H.Henry and D.V.Lang, Phys.Rev. B 15, 989 (1977)
44. J.S.Blakemore, Phys.Rev. 163, 809 (1967)
45. L.D.Yau and C.T.Sah, Solid-State Electron. 17, 193 (1974)
46. B.Welz, Atomic Absorption Spectroscopy (New York 1976)
47. G.E.Pake and T.L.Estle, The Physical Principles of Electron Paramagnetic Resonance (W.A.Benjamin 1973)
48. G.Jones and J.Woods, J.Luminescence 9, 389 (1974)
49. G.Jones and J.Woods, J.Phys. D 6, 1640 (1973)
50. Z.K.Kun and R.J.Robinson, J.Electr.Mat. 5, 23 (1976)
51. R.J.Robinson and Z.K.Kun, Appl.Phys.Lett. 27, 74 (1975)
52. Y.S.Park and B.K.Shin, J.Appl.Phys. 45, 1444 (1974)
53. M.Yamaguchi,A.Yamamoto and M.Kondo, J.Appl.Phys. 48, 196 (1977)
54. J.W.Allen,A.W.Livingstone and K.Turvey, Solid-State Electron. 15, 1363 (1972)
55. M.E.Özsan and J.Woods, Solid-State Electron. 18, 519 (1975)
56. A.W.Livingstone,K.Turvey and J.W.Allen, Solid-State Electron. 16, 351 (1973)
57. L.Samuelson, PhD-Thesis (Lund 1977)
58. G.Björklund and H.G.Grimmeiss, Solid-State Electron. 14, 589 (1971)
59. S.Braun and H.G.Grimmeiss, Solid-State Commun. 12, 657 (1973)
60. C.H.Henry,H.Kukimoto,G.L.Miller and F.R.Merrit, Phys.Rev. B 7, 2499 (1973)
61. T.N.Morgan, J.Electr.Mat. 4, 1029 (1975)
62. T.N.Morgan, Phys.Rev.Lett. 40, 190 (1978)
63. G.B.Stringfellow and R.H.Bube, Phys.Rev. 171, 903 (1968)
64. J.W.Allen,M.D.Ryall and E.M.Wray, Phys.Status Solidi a 17, K101 (1973)
65. S.Braun,H.G.Grimmeiss and J.W.Allen, Phys.Status Solidi a 14, 527 (1972)
66. H.R.Szawelska and J.W.Allen, J.Phys. C 10, 2115 (1977)

Optical and electrical properties of the red copper center in ZnSe.

by

Christer Ovrén

Department of Solid State Physics, Lund Institute of Technology,

Box 725, S-220 07 LUND 7, Sweden

Abstract.

Emission and capture rates describing the optical and thermal transitions at a deep state in copper-doped ZnSe have been investigated using both photocapacitance techniques and photoconductivity measurements. The center investigated has previously been found to be introduced by Cu-doping and has been identified as the center responsible for the red copper luminescence in ZnSe. Optical and thermal emission rates were measured with a technique, in which the depletion region of a Schottky diode is kept constant during the measurements of transients. This permits the use of samples in which the deep level doping is comparable to the shallow doping, giving higher signals than in the types of samples used conventionally. By comparing cross sections obtained from the optical quenching of photoconductivity at different temperatures with the spectra obtained from junction measurements, it is found that the electric field in the junction does not introduce any broadening of the absorption edge. The capture cross section for the recombination of electrons from the conduction band into the center has been measured in the temperature range 77-200 K and found to be $2.4 \cdot 10^{-20}$ cm^2 at 200 K. The data obtained are analysed using the configuration coordinate

model, which is found to describe many features of the experimental data. The constant which characterizes the coupling to the lattice and the energy of the interacting phonons are estimated from the luminescence spectrum. The shape of the optical cross sections for absorption processes can be understood if it is assumed that not only optical excitations from the center directly into band states contribute, but also excitations to band states via discrete energy levels.

Optical and electrical properties of the red copper center in ZnSe.

by

Christer Ovrén

Department of Solid State Physics, Lund Institute of Technology,

Box 725, S-220 07 LUND 7, Sweden

I. Introduction.

The optical and electrical properties of many semiconductors can be influenced by doping with Cu. In ZnSe, Cu-doping gives rise to two emissions in photoluminescence[1, 2], the so called "Cu-red" and "Cu-green" emissions. Cu-doping also reduces the free carrier concentration in n-type ZnSe[3], and Cu-doped ZnSe is photoconductive[1]. An energy level in ZnSe which has been detected in photocapacitance studies, has recently been identified[3] as caused by Cu. This state has a threshold energy at about 0.68 eV for optical excitation of electrons from the valence band into the level and it was also shown[3] that this energy state is responsible for the Cu-red emission in ZnSe. Cu is easily introduced both intentionally and unintentionally in ZnSe during the growth and device fabrication processes and Cu is present in the material[3] unless it is carefully purified. Thus a good knowledge of the properties of Cu-doped ZnSe is valuable.

In this paper a study of Cu-doped ZnSe is presented, from which excitation and recombination parameters for the Cu-red center are obtained. The optical and thermal emission rates for this center are remeasured (section III) in a larger temperature range with better samples and

improved measurement techniques. The capture constant for the capture of electrons from the conduction band into the Cu-red level is measured (section IV) in the temperature range 77-200 K. By photoconductivity investigations it is shown (section V) that the electric field in the junction does not effect the shape of the optical cross sections and their temperature dependence. The excitation and recombination parameters for the center are analysed (section VI) within a configuration coordinate model describing the electron-phonon interaction in the transitions at the impurity.

II. Crystal growth and Schottky barrier fabrication. Material characterization.

The ZnSe crystals were grown by the sublimation method[7]. The high-ohmic asgrown crystals were treated in highpurity liquid Zn. This treatment has the effect of making the crystals low-ohmic[8], which is believed to be due to the out-diffusion of compensating impurities such as Cu. The outdiffusion of Cu has been shown experimentally with the aid of the radiotracer method[3,8]. After these first two treatments in liquid Zn, the crystals were subjected to a third aftertreatment in a mixture of liquid Zn and Cu, containing 1% of Cu. It has previously been shown[3] with radiotracer technique that this treatment introduces Cu into the crystals. Using this method and cutting off parts of the crystal, the Cu-doping was found to be homogeneous.

The properties of the material were investigated using different measuring techniques as described in a previous paper[3]. The photoluminescence of the (Zn,Cu)-treated crystals showed the well-known red Cu-emission[1,2] both with extrinsic and intrinsic excitation.

Schottky barriers were fabricated by evaporation of gold on to the crystals. The properties and fabrication[9] of these diodes have been described earlier.

III. Emission rates and impurity concentrations.

Current and capacitance measurements with pn-junctions and Schottky barriers are commonly used for investigations of deep impurities. A survey over these methods has been given recently in a review paper[10]. With Schottky diodes, one is restricted mainly to transients measurements, since in the case of capacitance investigations, the steady-state capacitance change alone is not enough to extract the emission rates [5]. Using current measurements, the transient behaviour offers a possibility to separate out the contribution to the current from the carriers, which have been photoexcited from the metal into the semiconductor, thus obtaining the response from the deep levels only[5]. Junction measurements are usually carried out with material with moderate deep level doping, that is with material where the condition $N_{Deep} << N_{Shallow}$ is fullfilled. If this is not the case, current and capacitance transients obtained are not simple exponential functions, basically due to a too large change of the width of the depletion region of the junction during the transients. When measuring capacitance the condition $N_{Deep} << N_{Shallow}$ implies that a small change in the capacitance of the diode has to be measured. Using current measurements, the condition $N_{Deep} << N_{Shallow}$, together with realistic values for shallow doping and junction areas, means that rather small currents normally are obtained. Furthermore, for current transients the condition[5], $\tau \cdot I(t=0) = \text{constant}$, implies that if the current is increased, e g by using a higher light intensity, the time-constant in the transient

becomes correspondingly smaller, giving rise to increasing measuring problems.

In order to improve the experimental conditions, the investigations presented in this paper are carried out with Schottky diodes fabricated on material with the deep level doping, N_{TT}, nearly equal to the shallow level doping, N_D. To remove the difficulties discussed above, the measurements are performed in such a way that the depletion region of the diode is constant during the transients[11,12]. This is accomplished by a feedback system from the capacitance meter, keeping the capacitance constant.

The experimental set-up is shown in figure 1. The capacitance meter employed, was a Boonton 72 BD and for the feed-back amplification a Keithley 427 current amplifier with variable amplification and damping was used. For a certain capacitance, the voltage V_C is set so that the point between the two resistors, R, is approximately at zero voltage. A change in the capacitance of the diode will produce a voltage at the input of the amplifier. The corresponding output voltage is added to the bias of the diode so that the capacitance is restored to its original value.

The principles of the measurement are shown in figure 2 and 3. Figure 2a is the band diagram of a Schottky barrier on a n-type semiconductor with an acceptorlike deep impurity ($N_{TT} < N_D$). In the region, W_o, nearest to the neutral material the deep levels are filled with electrons because of recombination due to the tail of free carriers extending from the neutral region[13,5]. In the remaining part, $W-W_o$, of the space-charge region, the concentration of levels, n_T, that are occupied, is determined by the emission rates.

It is clear that $0 \leq n_T \leq N_{TT}$. Figure 2b shows the space-charge, $\rho(X)$, when all the deep levels are filled with electrons ($n_T = N_{TT}$) and figure 2c shows the space charge for an arbitrary value of n_T. The electrical field in the space charge region as calculated from Poissons equation, is for $0 < X < W - W_o$

$$E(X) = \frac{e(N_D - n_T)}{\varepsilon\varepsilon_o} X + \frac{eN_{TT}W_o}{\varepsilon\varepsilon_o} - \frac{eN_DW}{\varepsilon\varepsilon_o} + \frac{en_T}{\varepsilon\varepsilon_o}(W - W_o) \qquad (1)$$

and for $W - W_o < X < W$

$$E(X) = \frac{e(N_D - N_{TT})}{\varepsilon\varepsilon_o}(X - W) \qquad (2)$$

and is shown in figure 2d.

The voltage drop over the junction is obtained by integrating the electric field,

$$V - V_R = \int_o^W E(X)\,dX = \int_o^{W-W_o} E(X)\,dX + \int_{W-W_o}^{W} E(X)\,dX = I_1 + I_2 \qquad (3)$$

Since the capacitance of the diode is kept constant, it follows that the total depletion width, W, is constant, and since W_o is independent of the reverse voltage[13, 5], the two integrals can be written as $I_1 = c_0 \cdot n_T + c_1$ and $I_2 = c_2$. Thus, the change in voltage needed to keep the capacitance constant, when the occupancy of the deep centers is changed, is proportional to n_T. Hence,

$$\Delta V(t) = \text{constant} \cdot n_T(t) \qquad (4)$$

Equation 4 is valid also in the case of a donor-like deep impurity.

Figure 3 shows the capacitance against voltage characteristic ($1/C^2$ vs V_R) for the Schottky diode used in the experiments. The diode temperature was 204 K, and at this temperature the thermal emission rates for electrons and holes at the center can be neglected (Section IIIb). Curve A is obtained by illuminating the sample with light of photon energy equal to 2.48 eV at each voltage before measuring the capacitance. It has previously been shown[5], that for this photon energy, the optical cross sections σ_n^o and σ_p^o are approximately equal for the center investigated here. Thus, measuring curve A, the space charge is as in figure 2c with $n_T = \left(e_n^o / (e_n^o + e_p^o)\right) \cdot N_{TT} \approx (1/2) \cdot N_{TT}$. Curve B is obtained when the capacitance is being measured after illuminating the sample with light of photon energy 0.83 eV. This illumination completely fills the deep centers with electrons, because the level is located in the lower half of the bandgap[5]. Curve B is consequently measured with a space-charge as in figure 2b. From figure 3 it is easily seen that by keeping the capacitance constant, e g as shown by the dashed line in the figure, a large voltage change, about 4 volts in this case, can be obtained after illumination with light of different photon energies.

Figure 4 shows a typical voltage transient. The change in voltage is of the same order as the total voltage over the diode and the time-dependence is exponential. During the measurement the capacitance was kept constant within 0.5 percent.

From the capacitance-voltage characteristic (figure 3), the deep and the shallow doping concentration can be calculated. With the space charge shown in figure 2b we have

$$\frac{2}{A^2 e\varepsilon\varepsilon_o} \frac{dV_R}{d(1/C^2)} = N_D - N_{TT} \qquad (5)$$

where A is the surface area of the diode. Equation 5 and curve B of figure 3 then give $N_D - N_{TT} = 1.8 \cdot 10^{16}$ cm^{-3}. With the space charge shown in figure 2c and with $n_T = (1/2)N_{TT}$, the following relation is obtained[11, 14, 15] for the case of homogeneous doping

$$\frac{2}{A^2 e\varepsilon\varepsilon_o} \frac{dV_R}{d(1/C^2)} = \left\{(N_D - N_{TT}) + \frac{1}{2}N_{TT}\left(1 - \frac{W_o}{W}\right)\right\} \qquad (6)$$

The value of W_o for the deep level studied here can be taken as[5] $W_o = 0.17$ µm. With $dV_R/d(1/C^2)$ evaluated at 8 volt, W is 0.63 µm. Then from curve A of figure 3 we have $N_D - 0.64 \cdot N_{TT} = 2.7 \cdot 10^{16}$ cm^{-3}. Thus, $N_D = 4.3 \cdot 10^{16}$ cm^{-3} is obtained for the net shallow level doping and $N_{TT} = 2.5 \cdot 10^{16}$ cm^{-3} for the deep level concentration.

III a. Optical emission rates.

Although two emissions in photoluminescence are reported for Cu-doped ZnSe, no influence on the photocapacitance signals could be detected from other deep states than the Cu-red center. The Cu-green emission is quenched thermally with an activation energy of about 0.3 eV[1, 2]. The reason, that the corresponding energy state is not detected in photocapacitance measurements, may be that the electric field in the barrier gives rise to tunneling processes of electrons from the valence band into these states. In that case, it is not possible to create any change in the occupancy of these levels, which remains after the illumination is removed. (The electric field in the junction has a maximum value of about $1 \cdot 10^5$ V/cm).

Optical emission rates for the Cu-red center have been investigated previously with junction techniques[5, 3]. Due to the improvements of the experimental conditions, discussed above, it has been possible to carry out the measurements reported in this paper with greater accuracy. The investigations are also extended to lower temperatures, down to 40 K. This is possible because of the small ionization energy for shallow donors in ZnSe[16, 17]. Below 40 K, the measured capacitance starts to change drastically, due to the increase in the series resistance of the diode as the shallow levels are being filled. In the temperature range, 40-200 K, where the optical cross sections are measured, the thermal emission rates for the Cu-red center can be neglected (Section IIIb).

The optical cross section σ_p^o, for excitation of electrons from the valence band into the impurity level was measured by the following procedure:

1: Illumination with light of photon energy 2.48 eV. With this light, the occupancy of the centers in the inner part of the depletion region is determined by[5] two-step optical excitation processes and can be taken as $\frac{n_T}{N_{TT}} \approx \frac{1}{2}$. At the temperatures, where the measurements are carried out, the number of levels occupied with electrons remains constant for long times after the illumination is removed.

2: Illumination with "the measuring light" of photon energy $h\nu$, ($h\nu < E_C - E_{TT}$, see figure 2). The voltage transient, which is created as the empty centers are being refilled, is studied and σ_p^o is obtained from the time constant, τ, of this transient as[5]

$$\sigma_p^o = \frac{1}{\tau \cdot L} \tag{7}$$

where L is the photon flux.

The optical cross section σ_n^o for the excitation of electrons from the level into the conduction band was measured using the following technique:

1: Illumination with light of photon energy 0.83 eV. As the impurity levels studied are situated in the lower part of the bandgap[5, 3], they are filled with electrons by this light.

2: Illumination with "the measuring light" of photon energy $h\nu$. A fraction of the levels will be emptied and the corresponding voltage transient is recorded. σ_n^o is obtained from the voltage transient as[5]

$$\sigma_n^o \sim \frac{\Delta V}{\tau . L} \qquad (8)$$

The spectral dependence of the two cross sections at different temperatures is shown in figure 5, 6, 7 and 8 in linear and logaritmic plots. The cross sections have been related to each other by measurements with the same photon flux. For σ_p^o the absolute value is shown. The main feature of both cross sections is that they have a peak at the low energy side of the spectrum, which broadens and decreases with increasing temperature. No structure could be noticed in the curves.

III b. Thermal emission rates.

The thermal emission rate, e_p^t for the excitation of electrons from the valence band into the deep levels was measured in the following way:

1: Illumination with light of photon energy 2.48 eV, creating an occupancy number, n_T/N_{TT}, less than one.

2: After the light-source is turned off, the emptied levels are thermally refilled and the corresponding voltage transient is observed. Because

$e_p^t \gg e_n^t$ for the center investigated here, e_p^t is given by

$$e_p^t = \frac{1}{\tau} \tag{9}$$

where τ is the time constant of the voltage transient. In figure 9 the thermal emission rate e_p^t is plotted semilogaritmically as a function of the inverse temperature. For comparison the data from an earlier investigation[5] are shown in the diagram. The slopes of the two curves are the same. The new data are obtained with a more straight-forward technique using a better sample. This, or the uncertainty in determining the absolute temperature of the diode might be the reason for the discrepancy in absolute values.

IV. Capture cross sections.

The cross section σ_n, describing the capture of electrons from the conduction band into the Cu-red level was measured by applying short voltage pulses in the forward direction to the reverse-biased Schottky diode and monitoring the resulting change in the diode capacitance[18]. The investigations were made in a temperature range where the thermal emission rates are negligible.

The set-up, which was used, is a fast capacitance bridge of the construction described in ref 19 (figure 10). The capacitance part of the signal was picked out by adjusting the delay-line, so that the change in the output signal was maximum for a small change in the diode bias. In order to be able to detect small variations of the capacitance (see below), part of the diode capacitance was out-compensated, either by a net in parallell to the diode or simply by a DC-voltage at the output.

Since the Cu-red level is located in the lower half of the bandgap, the initial occupancy of the centers was arranged by illumination. The pulses applied to the diode were always smaller than $|V_R|+|V_D|$, so that the forward current during the pulses was small. The principle of the measurements is illustrated in figure 11. The initial condition is determined by illumination with light of photon energy 0.83 eV, filling all Cu-red centers with electrons. Illumination with light of photon energy 2.48 eV, increases the capacitance, because the impurity level is located in the lower half of the bandgap. The capacitance remains at this value for long times, in the temperature range of the measurements. A subsequent illumination with the 0.83 eV light-source causes the capacitance to decrease again to its original value. If, after the illumination with the 2.48 eV light-source, the voltage over the diode is reduced for a short time, recombination takes place and the capacitance decreases. After a sufficient number of pulses, the capacitance reaches its initial value, if the depletion region width during the pulses can be neglected.

Because the concentration of the deep impurity is of the same order as the shallow doping, a non-exponentional time-dependence of the capacitance is obtained when the pulses are applied, as discussed above. However, if the charge on only a small fraction of the deep centers is varied, the corresponding change of the capacitance is small, with an exponential time dependence (figure 12). This can be accomplished either by illuminating with light of a smaller photon energy than 2.48 eV (figure 7) or by reducing the time for the illumination. The second alternative was used here because the influence on the signal caused by other deep centers eventually present in the sample should then be smaller.

A typical experimental curve used for the determination of c_n is shown in figure 12. The length of the pulses was 100 μsec and the diode temperature 204 K in this case. In order to verify that the time-constant, τ, is independent of the length, T_{pulse}, of the pulses, this was varied between 500 nsec and 100 μsec. No change of τ was observed.

From the relation[18]

$$\frac{1}{\tau} = c_n \cdot n \qquad (10)$$

the capture constant, c_n, can be calculated if the free carrier concentration, n, is known. The capacitance-voltage characteristic (figure 3) gives $N_D - N_{TT} = 1.8 \cdot 10^{16}$ cm^{-3}, which is the carrier concentration if the shallow donors are completely ionized. The free carrier concentration as a function of temperature can be obtained from Hall and dark conductivity measurements. Such measurements[20] with ohmic samples fabricated of the material used for the Schottky diodes give as values for n, $1.4 \cdot 10^{16}$ cm^{-3} at 200 K and $0.4 \cdot 10^{16}$ cm^{-3} at 77 K. The values and the temperature dependence of n are in good agreement with the results obtained from the capacitance measurements. Taking then $n = 1.4 \cdot 10^{16}$ cm^{-3}, c_n can be calculated from (10) as $c_n = 2.2 \cdot 10^{-13}$ cm^3 s^{-1}. Together with the mean thermal velocity $\bar{v}_{th} = \sqrt{\frac{8kT}{\pi m}} = 0.9 \cdot 10^7$ cm/s, the value of the capture cross section obtained, is $\sigma_n = 2.4 \cdot 10^{-20}$ cm^2 at 200 K.

Measurements at different temperatures show that within the experimental accuracy, about 10 %, the time constant, τ, is independent of temperature in the temperature region, 77 K < T < 204 K, were measurements were made. Together with the variation of n mentioned above and the thermal velocity, $\sigma_n = 1.4 \cdot 10^{-19}$ cm^2 is obtained for the capture cross section at 77 K.

To measure the capture cross section for holes, σ_p^t, and its temperature-dependence, holes have to be injected in the depletion region. One possible way to do this is to illuminate the structure from the rear with intrinsic light[21]. The thinnest structure which could be fabricated, was about 5-10 μm thick under the Schottky-contact and since the diffusion-length for holes in this material is rather small ($L_p \leq 0.1$ μm), the concentration of holes has decreased several orders of magnitude at the depletion region edge. When excited in the UV region, the material shows the selfactivated emission. This light has a long penetration depth in the material and can give rise to two-step excitations over the Cu-red center in the depletion region, contributing to the time constant of a detected capacitance change. Thus, to use this method for measurements of hole capture cross sections in ZnSe, the thickness of the sample should be of the same order as the diffusion-length.

V. Photoconductivity measurements.

With junction techniques, optical cross sections are measured in the presence of a high electric field. Measurements with different reverse biases have shown that the cross section edges broaden with increasing electric field for some deep centers, e g Si:S[22], Si:Zn[23] and GaP:O[24]. Also, a comparison of results obtained from measurements in bulk material with data from junction experiments, for GaP:O[25], shows a difference in the edge region between the optical cross section spectra obtained by the two methods. On the other hand, such a comparison for GaP:Cu[26] shows no influence on the spectra of the electric field in the junction.

In order to establish if there is a field-dependence of the optical cross sections for the Cu-red center in ZnSe, photoconductors of Cu-doped material were investigated. The samples used, were grown with the sublimation method and homogeneously Cu-doped either by the addition of $CuCl_2$ during the growth process, or by an aftertreatment in a solution of 90 % Zn and 10 % Cu. The optical and electrical properties of the samples obtained by these two methods were very similar. In photoluminescence, the red and the green Cu-emissions are obtained, when the crystals are excited with light of wavelength 3650 Å at 77 K. The relation between the intensity of the green and the red band under these conditions, is about 10/1 in these high-ohmic crystals. The corresponding ratio for the low ohmic material used for the junction measurements was always less than 1/10.

The photoconductivity properties of the samples agree well with what has been reported earlier for Cu-doped material[1, 27]. The photoconductivity increases appreciably for photon energies larger than about 2.2 eV. The photoconductivity response is also temperature dependent as reported earlier[1, 27]. Below 40 K, the photoconductivity decreases exponentially with an activation energy of about 0.01 eV. Optical quenching of the photoconductivity was observed both with extrinsic and intrinsic primarily excitation.

The relation between the quenching of photoconductivity and optical emission rates is in general rather complicated. Because the capture cross section for electrons is many orders of magnitude smaller than the capture cross section for holes for the Cu-red center (section IV and VI), we assume that the quenching is due to excitation of holes from the Cu-red center into the valence band, moving part of the

recombination to other channels and resulting in a decrease of the life-time for the excited electrons. With photon energies of the secondary light (which causes the quenching) smaller than half the bandgap, the magnitude of the quenching depends explicitly on this light only through the optical emission rate e_p^o, which can be expressed as the product of the optical cross section σ_p^o and the photon flux L. This can be used to obtain a simple relation between the measured signal and the cross section[28]. Using a feedback system, the measurements are carried out in such a way that the quenching is kept constant when the photon energy of the secondary light source is varied. Constant quenching can be obtained if the photon flux L of the secondary source varies in such a way that

$$e_p^o = \sigma_p^o \cdot L = \text{constant} \qquad (11)$$

Then, by plotting the reciprocal of the photon flux versus the photon energy, the spectral distribution of σ_p^o is obtained. Figure 13 shows the result of such measurements at two different temperatures. The same spectra are obtained with the two types of samples described above, either with intrinsic or extrinsic primary excitation. In the edge region there is good agreement between the data obtained from junction and from bulk measurements. At higher photon energies the quenching data deviate from the photocapacitance spectra, presumably due to other centers affecting the quenching measurement. (In contrast to junction measurements, photoconductivity quenching is not selective for a particular center, but all centers with favourable values of the excitation and recombination parameters contribute to the signal).

The data presented in figure 13 show that in the region of the measurements, the electric field in the Schottky diode is not causing any broadening of the optical cross section σ_p^o for the Cu-red center.

VI. Discussion.

The two optical cross sections, σ_n^o and σ_p^o (figure 5-8), have a temperature dependence which consists mainly of a broadening of the absorption edges with increasing temperature and slight decreases of the peaks at the low energy edges as the temperature increases. The red copper luminescence has been interpreted[1,27] as being due to the recombination of electrons from the conduction band into a Cu-level at temperatures above 40K and as being due to the recombination of electrons from shallow levels (located at about 0.01 eV below the conduction band) into the center at lower temperatures. These processes give rise to a broad emission[1,2,27], the width of which increases when the temperature increases. Such broad emissions occur frequently in the II-VI compounds and are usually explained in terms of electron-phonon interactions in the optical transitions.

One model used to describe such interactions is the so-called "configuration coordinate model"[29-33], which was originally used to handle transitions between discrete energy levels, but which has also been applied to transitions between discrete levels and energy bands[34-38]. In this model, with the use of the adiabatic wave-function

$$\Psi(\vec{r},\vec{q}) = \varphi(\vec{r},\vec{q})\ \chi_e(\vec{q}) \qquad (12)$$

the matrix element which determines optical transitions can be separated into two parts[39] and

in the Condon approximation, one obtains[39]

$$|\langle\varphi_i|\tilde{H}_{rad}|\varphi_f\rangle|^2 \; |\langle\chi_{in}|\chi_{fm}\rangle|^2 \qquad (13)$$

$\varphi(\vec{r},\vec{q})$ is the electronic wave-function and $\chi_e(\vec{q})$ the wave-function describing the nuclei. $\vec{r}$ are the electron coordinates and $\vec{q}$ the lattice normal coordinates. Equation 13 describes optical transitions between the vibrational state n in the initial electronic state and the vibrational state m in the final electronic state. The total cross section for optical transitions between the two electronic states is obtained by summing over all possible combinations of initial and final vibrational states with proper thermal weight-factors for the initial states. If only one linear mode is considered, the optical cross section $\sigma^o(h\nu)$ for excitation processes can be taken as[32,34,36]

$$\sigma^o(h\nu)=\sum_{n=o}^{\infty}\sum_{m=o}^{\infty}\left[(1-e^{-\frac{\hbar\omega}{kT}})\cdot e^{-\frac{n\cdot\hbar\omega}{kT}}\cdot e^{-\lambda}\frac{m!}{n!}\lambda^{n-m}\left(L_m^{n-m}(\lambda)\right)^2\right]\cdot$$

$$\cdot\sigma_{el}^o(h\nu-(E_I-(n-m)\hbar\omega)) \qquad (14)$$

$L_m^{n-m}(\lambda)$ are associated Laguerre polynomials. n and m denote the vibrational states in the initial and final electronic state, respectively. The interaction is characterized by the constant λ and the energy, $\hbar\omega$, of the interacting phonons. E_I is the energy difference between the vibrational ground states in the two electronic states and σ_{el}^o the electronic cross section. At low temperatures, the factors multiplying σ_{el}^o can be described by a Poisson distribution[32].

In the semi-classical treatment[31,32], a Gaussian curve is obtained for these factors, with a half-width, W, varying with temperature as

$$W(T) = W(0) \left(\coth \left(\frac{\hbar\omega}{2kT} \right) \right)^{1/2} \qquad (15)$$

For linear modes, this treatment is applicable[32] when the constant λ is large, or when the energy $\hbar\omega$ of the interacting phonons is small compared to the temperature, kT.

The square of the half-width of the "Cu-red" luminescence is plotted as a function of temperature in figure 14. The values of the half-width are taken from reference 2 and were obtained with crystals which were Cu-doped by aftertreatment in a (Zn, Cu)-solution. The low-temperature value in figure 14 is taken from reference 27 and is the half-width for the pair-recombination. Assuming the electron-phonon interactions to be the same for the two types of transitions involved, the slope of the straight line in figure 14, together with the low-temperature half-width, gives a value of $\hbar\omega$=0.025 eV for the phonon energy. For large values of λ, the Poisson distribution can be converted into a Gaussian. This can be used to estimate a value of the constant λ, giving λ=9.

In order to use equation 14 for the description of σ_n^o and σ_p^o, an expression for the electronic cross section σ_{el}^o is needed. A calculation of optical cross sections for excitations between an energy level and an energy band requires a knowledge of the density of states in the band and of the wave-function for the bound

carrier. Symmetry effects[38,40,41,42] may also be important in determining the shape of optical cross sections.

Starting with σ_p^o, it can be assumed from a comparison between σ_p^o for the Cu-red center and σ_p^o for another deep center in ZnSe, investigated in reference 3, that the peak in σ_p^o for the Cu-red center is a property of this specific center. We therefore assume that not only excitations from the ground state for the hole into the valence band take place, but also excitations via another discrete energy level. As expressions[38] for σ_{el}^o, we therefore try

$$\sigma_{el}^o(h\nu) = C_o\, \delta(h\nu - E_o) + C_T \frac{(h\nu - E_T)^{1/2}}{(h\nu)^3} \qquad (16)$$

and

$$\sigma_{el}^o(h\nu) = C_o\, \delta(h\nu - E_o) + C_T \frac{(h\nu - E_T)^{3/2}}{(h\nu)^3} \qquad (17)$$

E_T and E_o are defined as indicated in the insert of figure 15. The expressions which describe optical excitations into band states in equation 16 and 17 can be regarded as representing the two cases when the cross section is dominated by contributions from conduction band and valence band Bloch functions in the impurity wavefunction[38], respectively. With the assumption of the same lattice-interaction for all the transitions involved, the optical cross section can now be calculated using equations 14, 16 and 17. Doing so, a structure appears on the low-energy peak of the calculated

curve. This is not seen experimentally, either in σ_p^o or in the emission spectrum. To eliminate this structure, an additional broadening, taken as $(1/\sqrt{\pi}\cdot\Delta)\cdot\exp-(\varepsilon/\Delta)^2$, is applied. In all the following calculations, a value of $\Delta = 0.02$ eV has been used, chosen just large enough to eliminate the structure. Such broadening effects might be due either to different environments for the centers in the crystal or could be due to interaction with other lattice modes. In this case, the electronic energies obtained from the calculations are slightly modified. In figure 15, calculations of σ_p^o using σ_{el}^o according to equation 16 (full line) and equation 17 (dashed line) are compared with experimental data obtained at 40 K (dots). It is clear from the figure and from the values used in the calculations to obtain the best fit, that the value of E_T obtained is very sensitive to the choice of σ_{el}^o. In order to determine threshold energies, calculated cross sections for optical transitions into band states are usually compared with experimental data obtained for photon energies near the threshold, where expressions such as equation 16 and 17 are expected to provide the best description. In this particular case, this is not possible because of the peak in the spectrum. Because σ_{el}^o according to equation 16 gives the better agreement with the experimental data, it is used for the calculations of the cross section at different temperatures (figure 16). The general trends in the temperature dependence of the spectrum are fairly well reproduced by the model. The electron-phonon interactions in the transitions between the ground state and the "excited" state are probably overestimated (See figure 16). Furthermore, it should also be observed that the same values of C_o and C_T have been used

at all temperatures. Absorption measurements might be useful to improve the model in these respects.

The origin of the energy level at E_T-E_o from the valence band cannot be established from these investigations. One possible explanation is that the level is due to an excited state for the hole, due to coulombic contributions in the impurity potential. The state might also arise from the splitting of a Cu d-state by the crystal field. The crystal field splitting parameter for Cu d^9 in II-VI compounds is about 0.7 - 0.75 eV[43-45].

The value of E_T=0.78 eV used in the calculation of σ_p^o could also be compared with the results obtained from the investigations of thermal emission rates. The detailed balance relation

$$e_p^t = g \cdot \bar{v}_{th} \cdot \sigma_p^t \cdot N_v \cdot e^{\frac{-E_T^t}{kT}} \qquad (18)$$

can be used to obtain an accurate value of the thermal ionization energy, E_T^t, if the temperature dependence of the capture cross section σ_p^t and of E_T^t is known[46]. $\bar{v}_{th}$ is the mean thermal velocity and N_v is the effective density of states in the valence band. g is a degeneracy factor. Equation 18 is valid also in the case with energy levels intermediate between the level studied and the band [47]. For the "Cu-red" center with an "excited" state, the capture cross section can show different temperature dependences[47], due to the characters of the various processes involved. If however, σ_p^t is taken to be independent of temperature, a plot of the logarithm of $e_p^t\, T^{-2}$ against T^{-1} gives a straight line with a slope corresponding to an energy of 0.72 eV. Using

this value, $\sigma_p^t \approx 1 \cdot 10^{-14}$ cm^2 can be estimated with g=1.

The optical cross section σ_n^o is also reproduced fairly well using equations 14 and 16 (Figure 17). Thus, also for this cross section, it has to be assumed that excitations between two discrete energy levels contribute to the spectrum. It cannot, however, be established from these measurements whether both these states are related to the Cu-red center.

In calculating σ_p^o and σ_n^o, the temperature dependence of the energy gap has not been taken into account. It can be seen from the spectrum of σ_p^o (Figure 6) that E_T for this transition seems to decrease as the temperature increases, although the accuracy of the measurement and of the model used is not enough to make a quantitative analysis.

A configuration coordinate diagram describing transitions between the center and the conduction band constructed from the parameters used in this paper for the calculation of σ_n^o, predicts the position of the luminescence peak for the Cu-red emission at about 1.96 eV. This can be compared with the experimental value, 1.94[3] eV at 77 K.

VII. Conclusions.

Many of the properties of the deep center investigated here can be described within a configuration coordinate model with a phonon energy and a coupling constant characterizing the interactions estimated from the luminescence spectrum. Using these parameters, the main features of the temperature dependence of the spectra of the optical cross sections for excitation processes can be explained. The shape of the cross section spectra can be understood if optical

excitations between discrete energy levels are taken into account as well as optical excitations directly into the bands. The absolute values of emission and capture parameters, reported here and their dependence of photon energy and temperature, can be used to calculate the influence of Cu-doping in different experiments. For example, the good photoconductivity properties of Cu-doped ZnSe can be understood as being due to the relatively large value of σ_n^o and the small value of σ_n.

Acknowledgements.

The author wants to thank Dr H Hartmann and Dr R Mach for the supply of ZnSe samples for these investigations. The discussions with Prof H G Grimmeiss, Dr W Ludwig and Dr R Mach are also gratefully acknowledged.

References.

1. G.B.Stringfellow and R.H.Bube, Phys.Rev. 171, 903 (1968)
2. G.Jones and J.Woods, J.Luminescence 9, 389 (1974)
3. H.G.Grimmeiss,C Ovrén,W.Ludwig and R.Mach, J.Appl.Phys. 48, 5122 (1977)
4. S.Braun,H.G.Grimmeiss and J.W.Allen, Phys.Status Solidi a 14, 527 (1972)
5. H.G.Grimmeiss,C.Ovrén and J.W.Allen, J.Appl. Phys. 47, 1103 (1976)
6. H.R.Szawelska and J.W.Allen, J.Phys. C 10, 2115 (1977)
7. M.Toyama and T.Sekiva, Jap.J.Appl.Phys. 8, 855 (1969)
8. M.Aven and H.H.Woodbury, Appl.Phys.Lett. 1, 53 (1962)
9. R.Mach,H.Treptow and W.Ludwig, Phys.Status Solidi a 25, 567 (1974)
10. H.G.Grimmeiss, Ann.Rev.Mater.Sci. 7, 341 (1977)
11. G.Goto,S.Yanagisawa,O.Wada and H.Takanashi, Appl.Phys.Lett. 23, 150 (1973)
12. J.A.Pals, Solid-State Electron. 17, 1139 (1974)
13. S.Braun and H.G.Grimmeiss, J.Appl.Phys. 44, 2789 (1973)
14. Y.Zohta, Appl.Phys.Lett. 17, 284 (1970)
15. Y.Zohta, Solid-State Electron. 16, 1029 (1973)
16. H.H.Woodbury and M.Aven, Phys.Rev. B 9, 5195 (1974)
17. G.Jones and J.Woods, J.Phys. D 9, 799 (1976)
18. C.H.Henry,H.Kukimoto,G.L.Miller and F.R.Merritt, Phys.Rev. B 7, 2499 (1973)
19. D.V.Lang, J.Appl.Phys. 45, 3014 (1974)
20. R.Mach and J.Maege, unpublished
21. B.Hamilton, Inst.Phys.Conf.Ser. 22, 218 (1974)
22. L.L.Rosier and C.T.Sah, J.Appl.Phys. 42, 4000 (1971)
23. J.M.Herman III and C.T.Sah, J.Appl.Phys. 44, 1259 (1973)
24. C.Ovrén, unpublished

25. L.Samuelson, PhD-thesis (Lund 1977)

26. P-O.Fagerström,H.G.Grimmeiss and H.Titze, Accepted for publication in J.Appl.Phys. (1978)

27. G.B.Stringfellow and R.H.Bube, J.Appl.Phys. 39,3657 (1968)

28. H.G.Grimmeiss and L-Å.Ledebo, J.Appl.Phys. 46, 2155 (1975)

29. K.Huang and A.Rhys, Proc.Roy.Soc. A204, 406 (1950)

30. M.Lax, J.Chem.Phys. 20, 1752 (1952)

31. D.L.Dexter, Solid State Phys. 6, 353 (1958)

32. T.H.Keil, Phys.Rev. 140, A601 (1965)

33. C.S.Kelley, Phys.Rev. B 6,4112 (1972)

34. J.M.Dishman and M.DiDomenico Jr, Phys.Rev. B 4, 2621 (1971)

35. H.Kukimoto,C.H.Henry and F.R.Merritt, Phys.Rev. B 7, 2486 (1973)

36. B.Monemar and L.Samuelson,Accepted for publication in Phys.Rev. (1978) and B.Monemar and L.Samuelson, J.Luminescence 12/13, 507 (1976)

37. A.A.Kopylov and A.N.Pikhtin, Sov.Phys.Solid State 16, 1200 (1975)

38. M.Jaros, Phys.Rev. B 16, 3694 (1977)

39. K.K.Rebane, Impurity Spectra of Solids (New York 1970)

40. D.M.Eagles, J.Phys.Chem.Solids 16, 76 (1960)

41. H.G.Grimmeiss,L-Å.Ledebo,C.Ovrén and T.N.Morgan, Proc.12:th Int.Conf.Phys.Semicond. (Stuttgart 1974)

42. J.M.Langer, Phys.Status Solidi b 47, 443 (1971)

43. I.Broser,H.Maier and H-J.Schulz, Phys.Rev. 140, A2135 (1965)

44. H.Maier and U.Scherz, Phys.Status Solidi b 62, 153 (1974)

45. E.M.Wray and J.W.Allen, J.Phys. C 4, 512 (1971)

46. O.Engström and H.G.Grimmeiss, J.Appl.Phys. 46, 831 (1975)

47. R.M.Gibb,G.J.Rees,B.W.Thomas,B.L.Wilson,B.Hamilton,D.R.Wight and N.F.Mott, Philosophical Magazine 36, 1021 (1977)

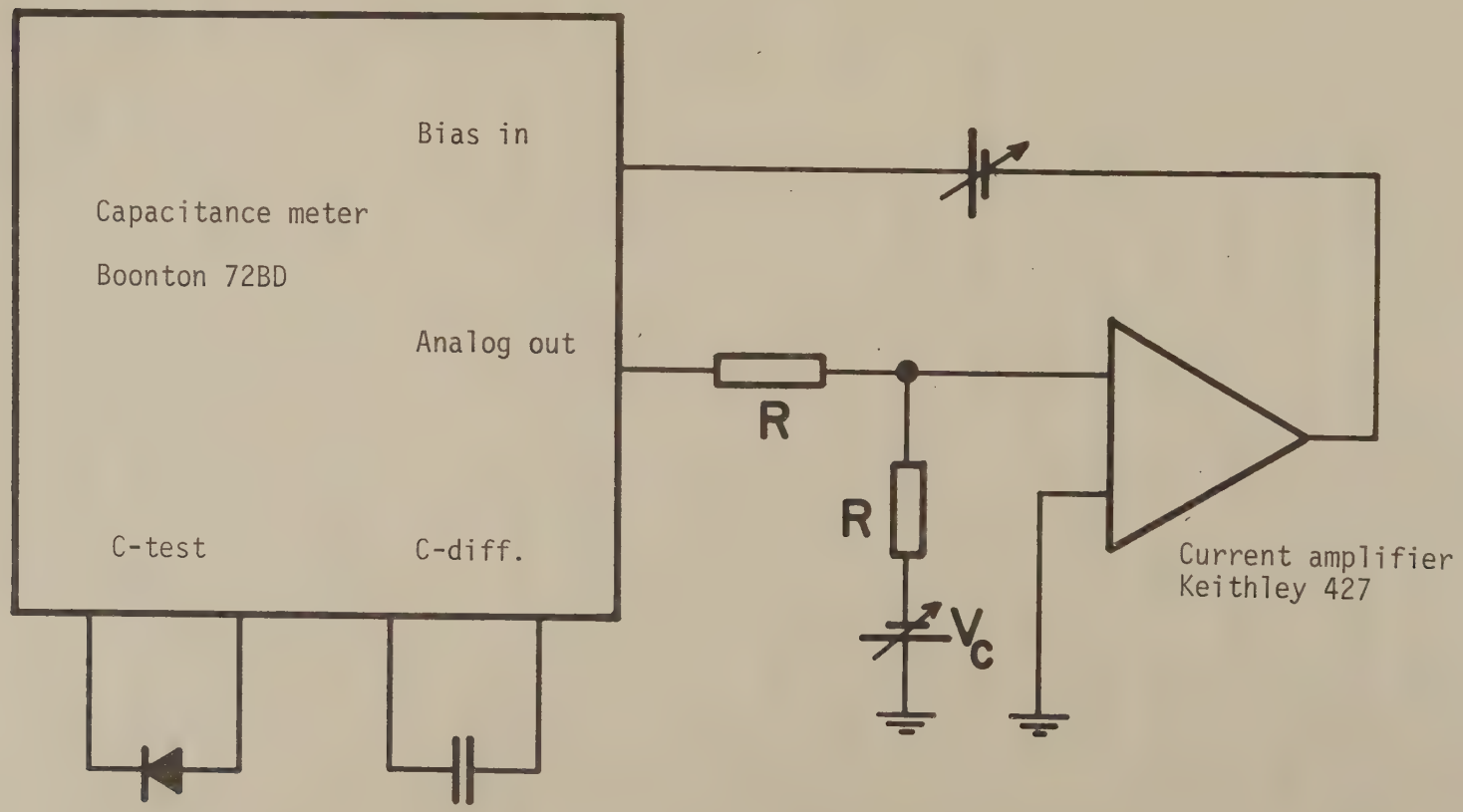

Fig 1

Schematic diagram of the set-up used for the measurements of optical and thermal emission rates.

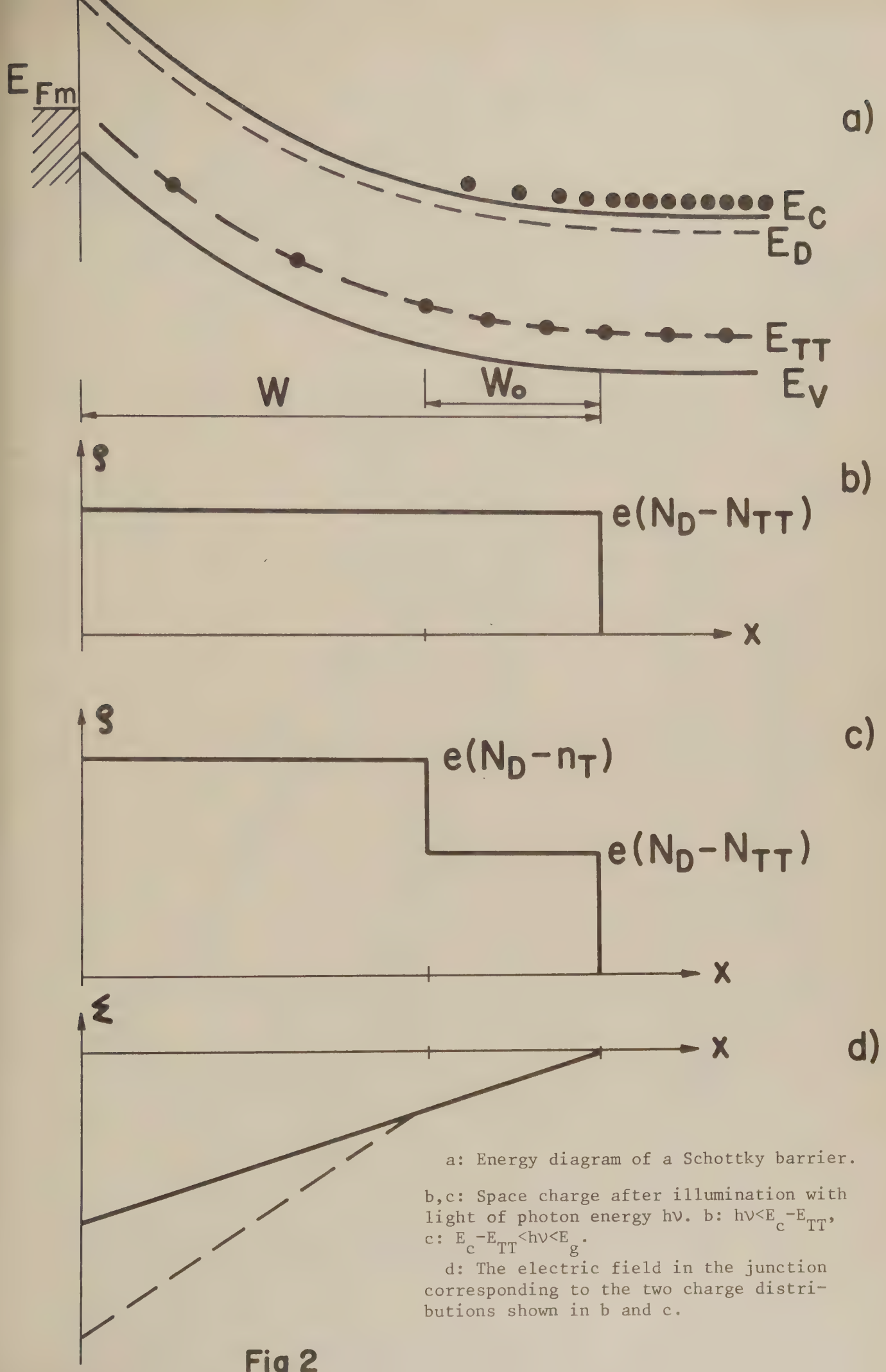

a: Energy diagram of a Schottky barrier.

b,c: Space charge after illumination with light of photon energy $h\nu$. b: $h\nu<E_c-E_{TT}$, c: $E_c-E_{TT}<h\nu<E_g$.

d: The electric field in the junction corresponding to the two charge distributions shown in b and c.

Fig 2

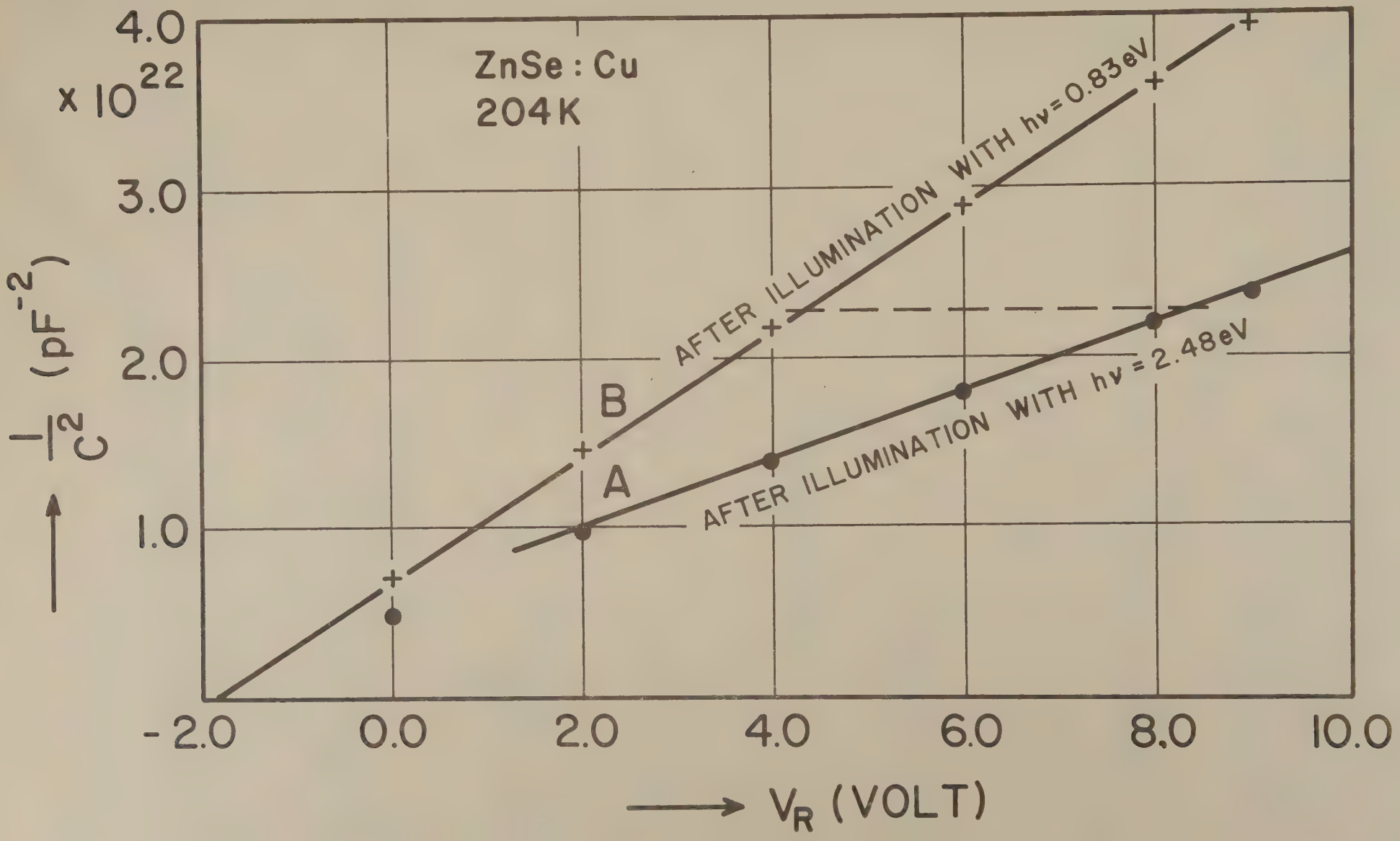

Fig 3

Capacitance-voltage characteristic for the Schottky diode used, measured after illumination with light of different photon energies.

Semilogaritmic plot of a typical voltage transient obtained. The diode is illuminated with light of photon energy 1.21 eV during the transient and was before the transient illuminated with light of photon energy 2.48 eV.

Fig 4

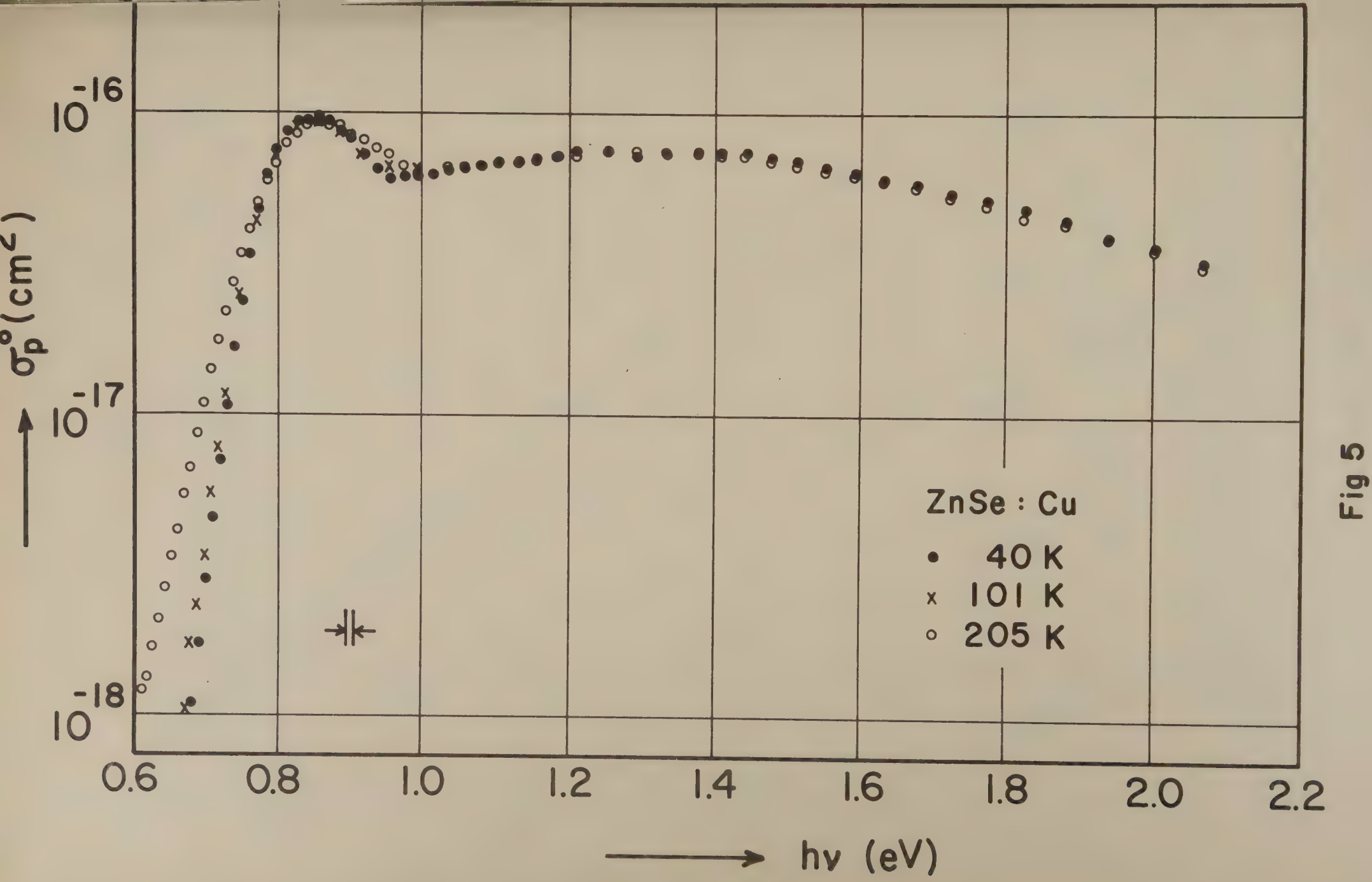

Fig 5

Spectra of the optical cross section σ_p^o at different temperatures.

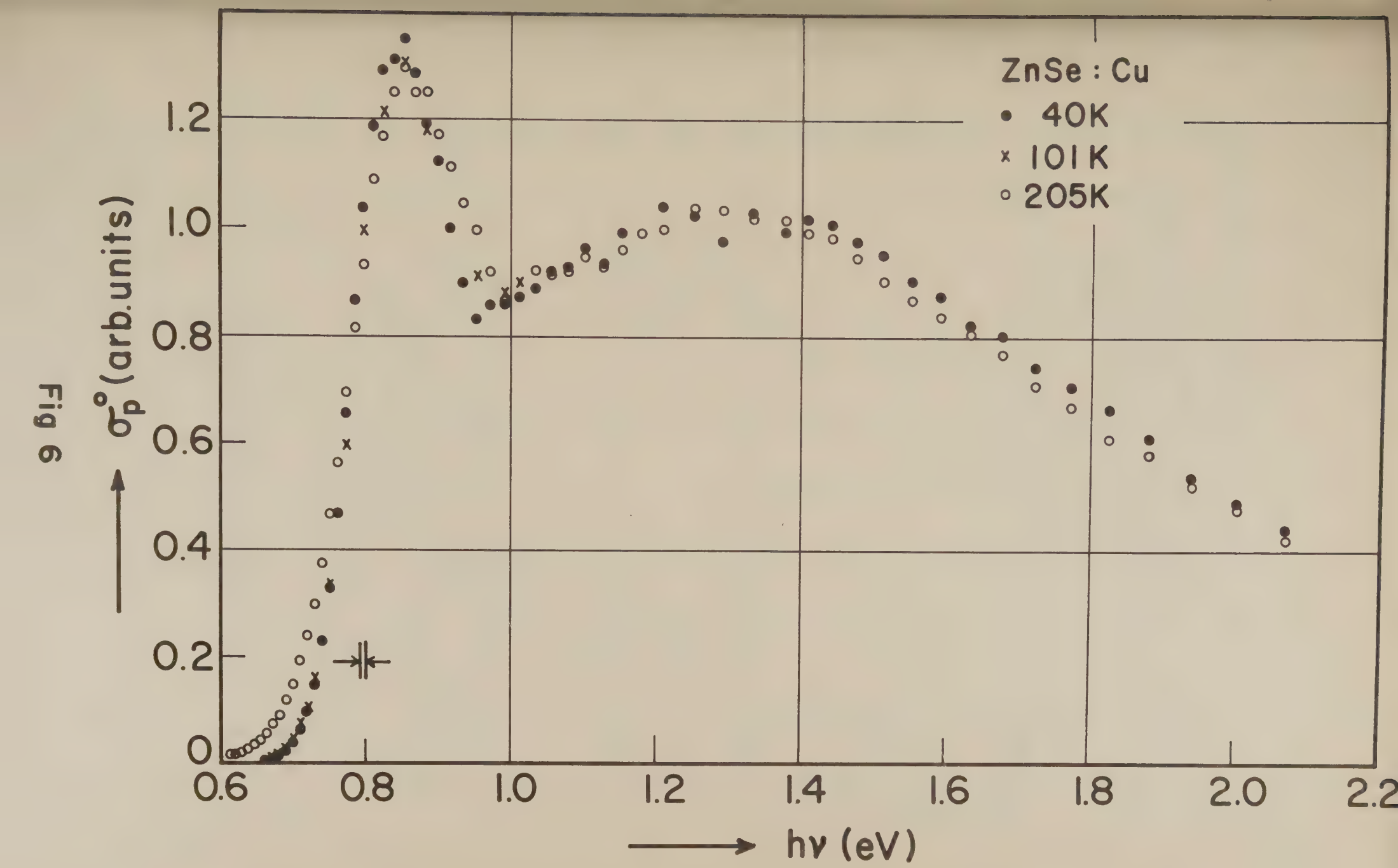

Fig 6

Spectra of the optical cross section σ_p^o at different temperatures.

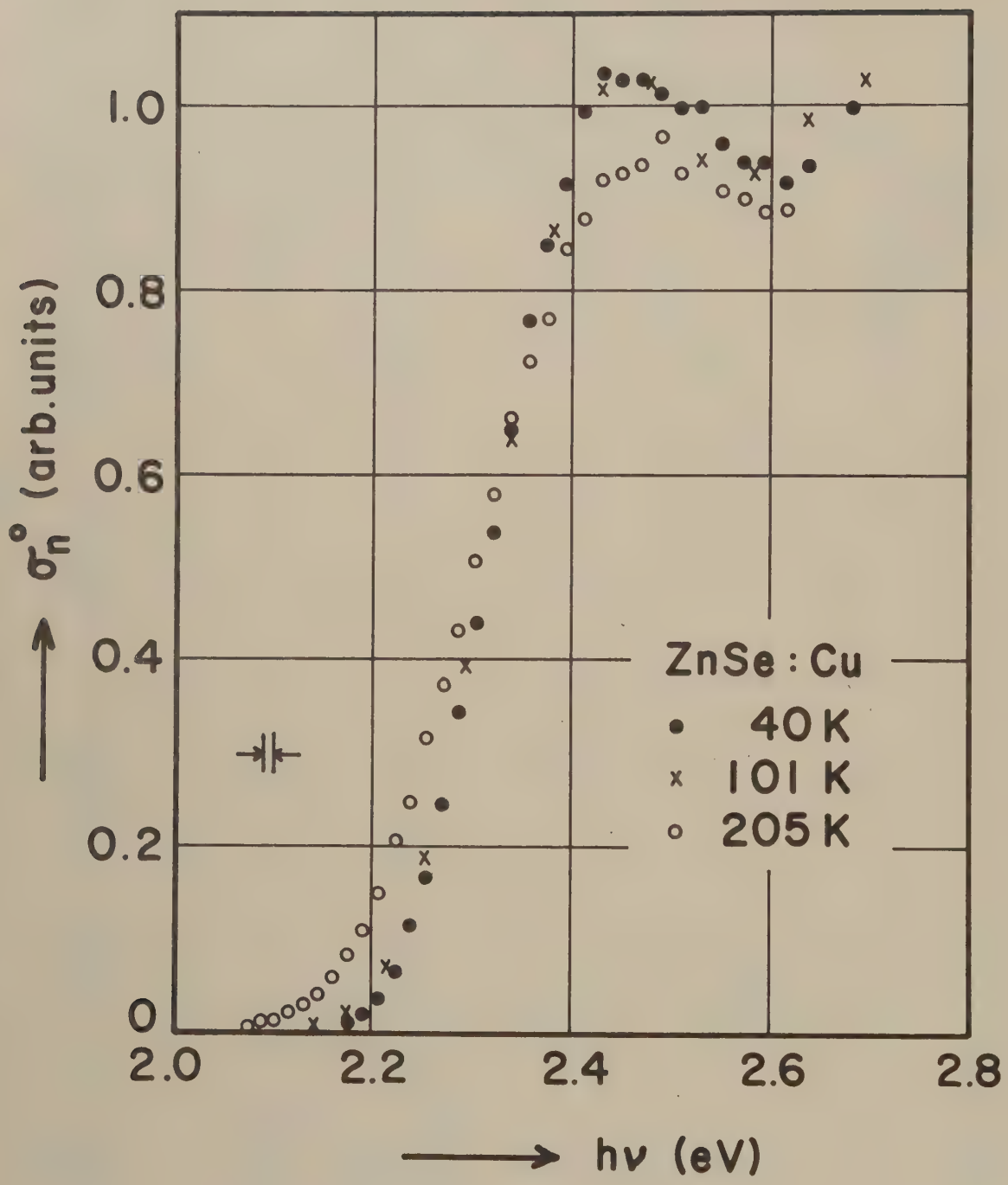

Spectra of the optical cross section σ_n^o at different temperatures

Fig 7

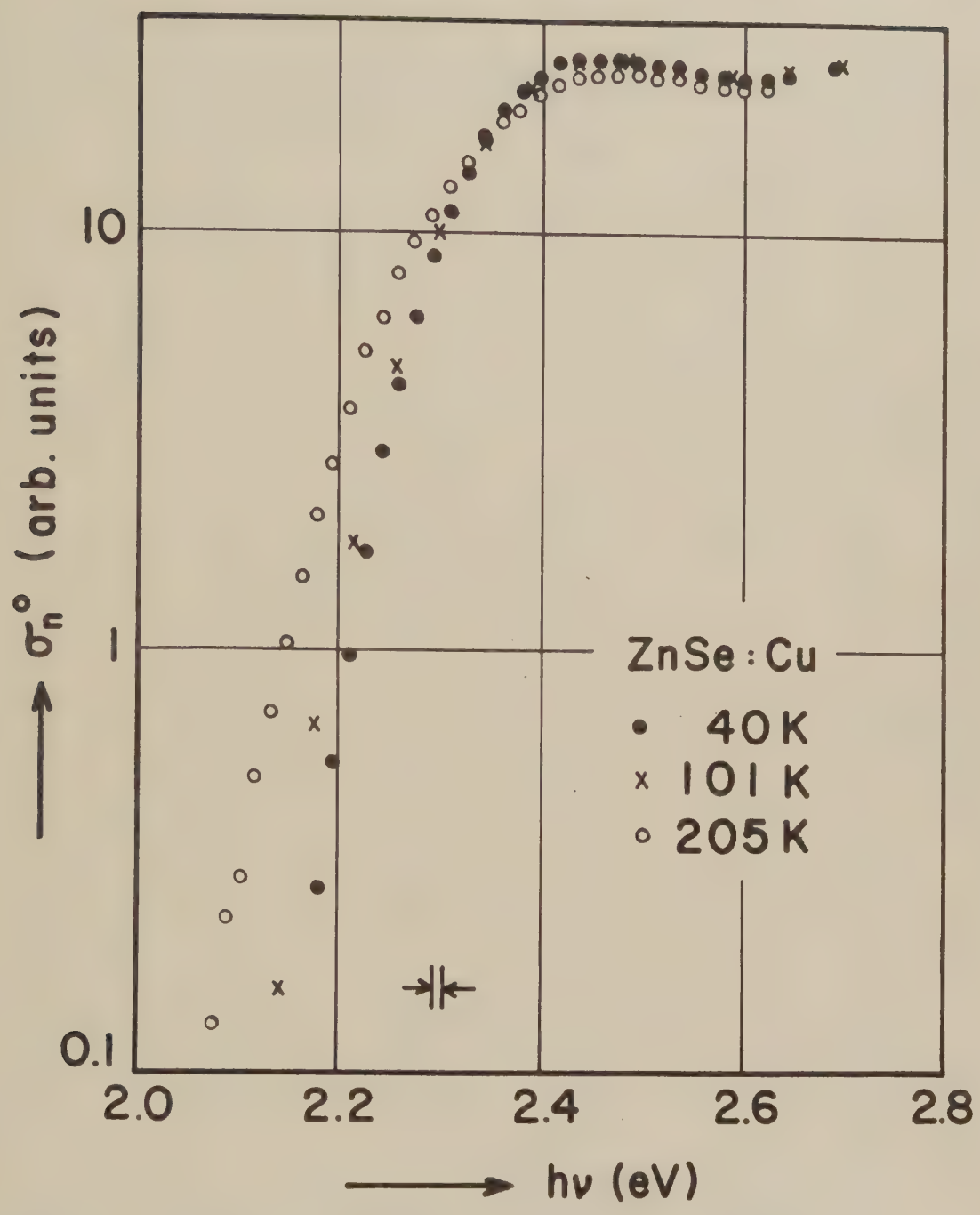

Spectra of the optical cross section σ_n^o at different temperatures.

Fig 8

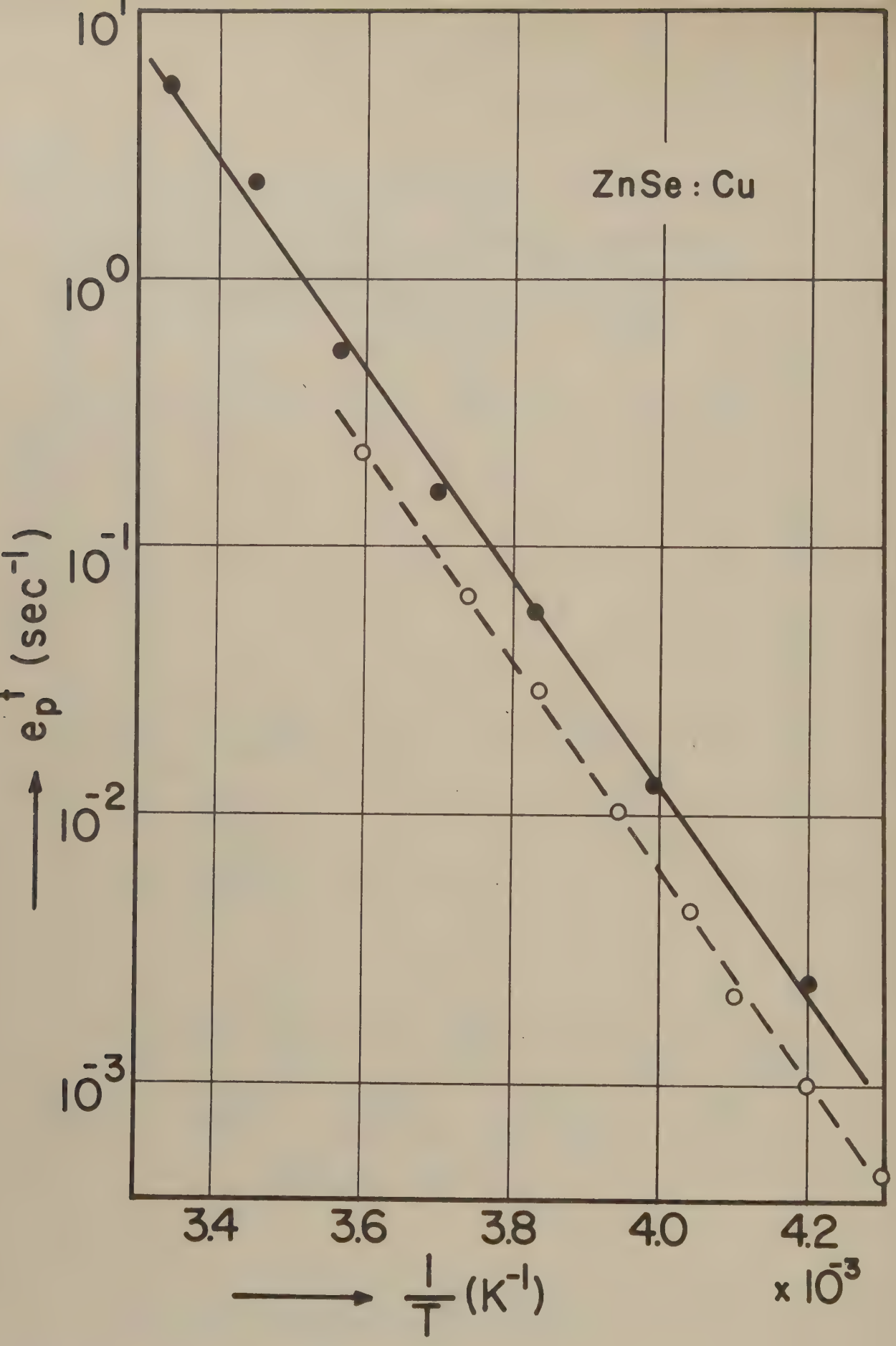

● The thermal emission rate e_p^t as a function of the inverse temperature. (o are data obtained from an earlier investigation, ref 5)

Fig 9

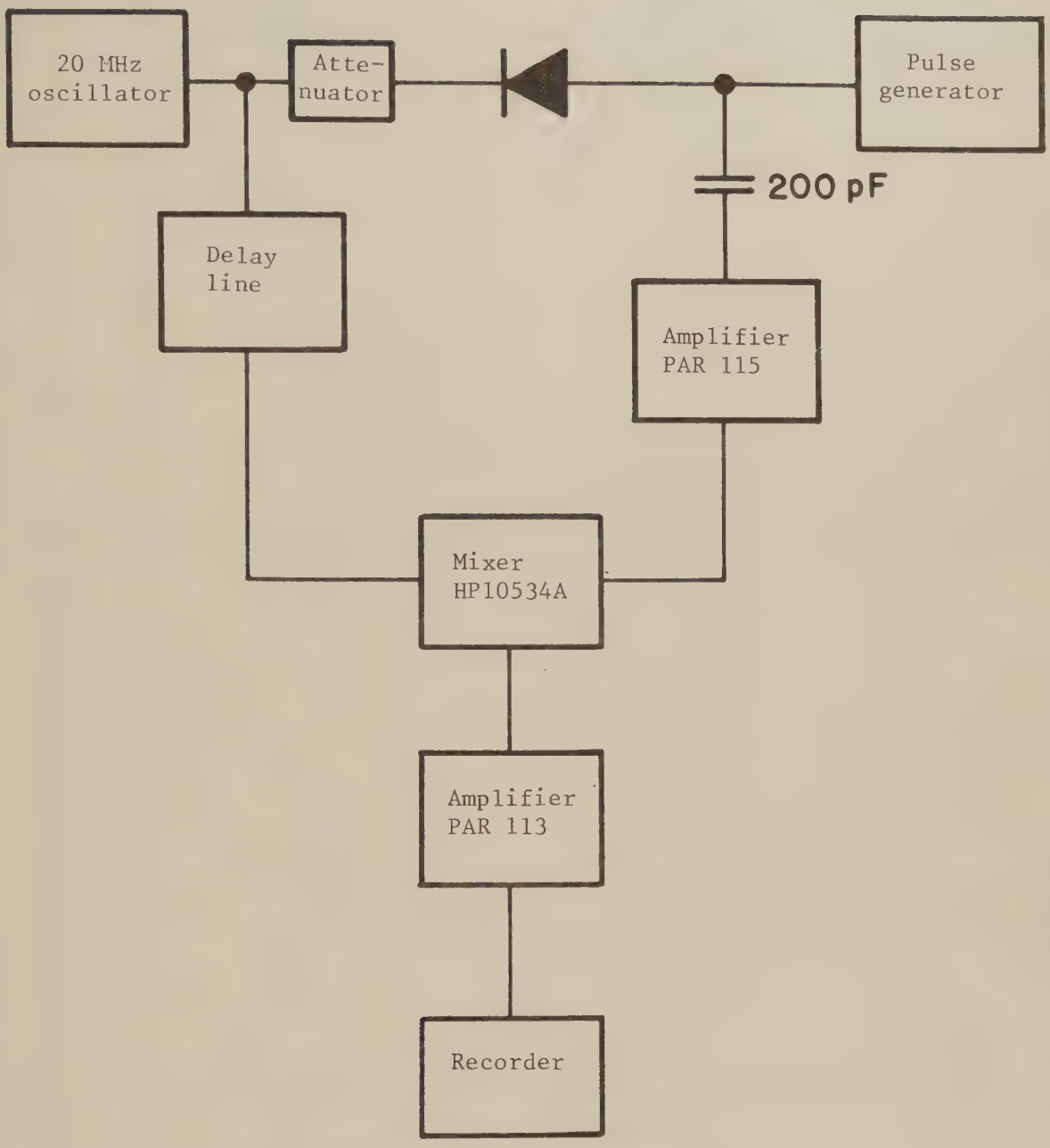

Block diagram of the capacitance bridge used for the measurements of the capture cross section σ_n.

Fig 10

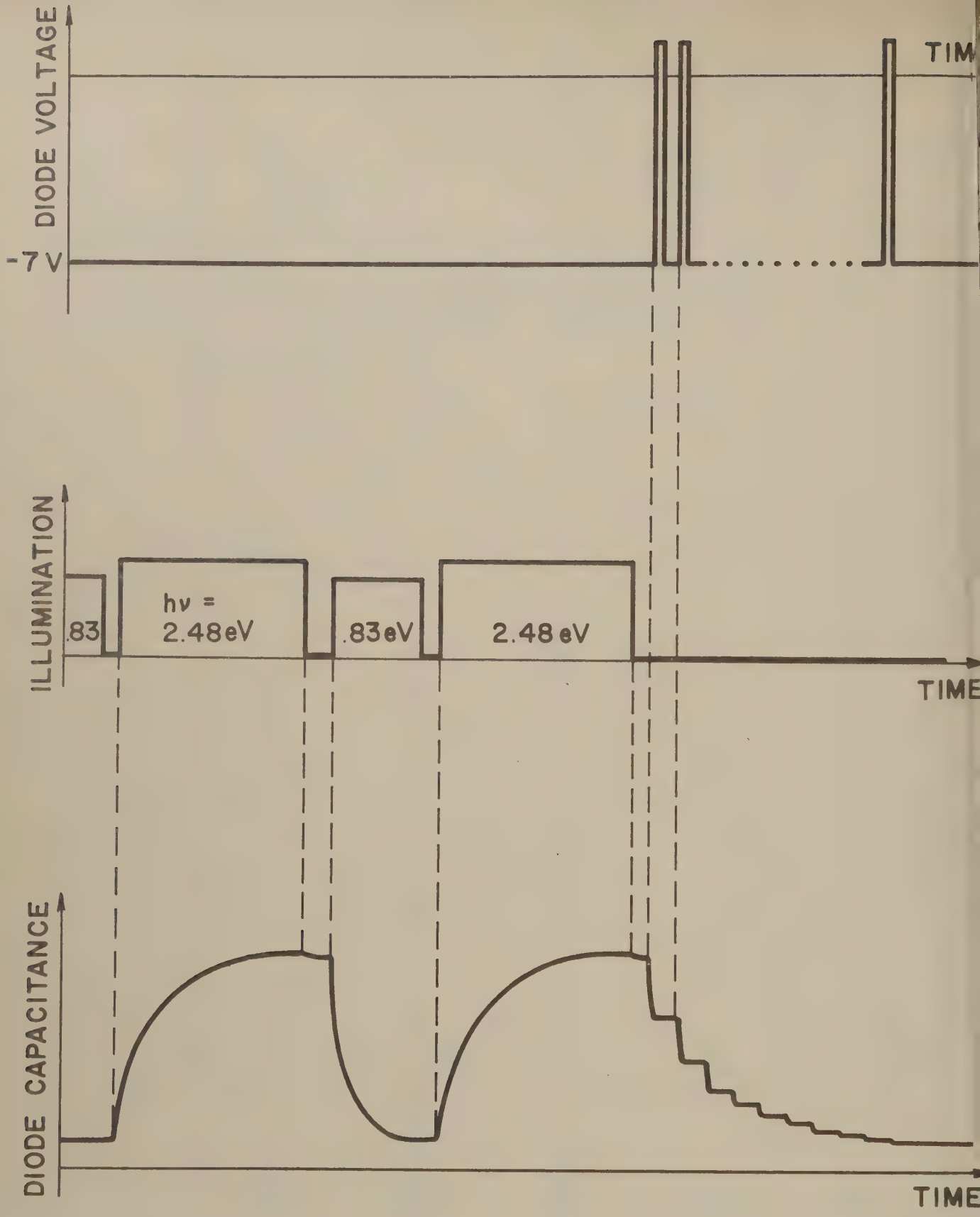

Schematic diagram illustrating the principle of the measurements of the capture cross section σ_n.

Fig 11

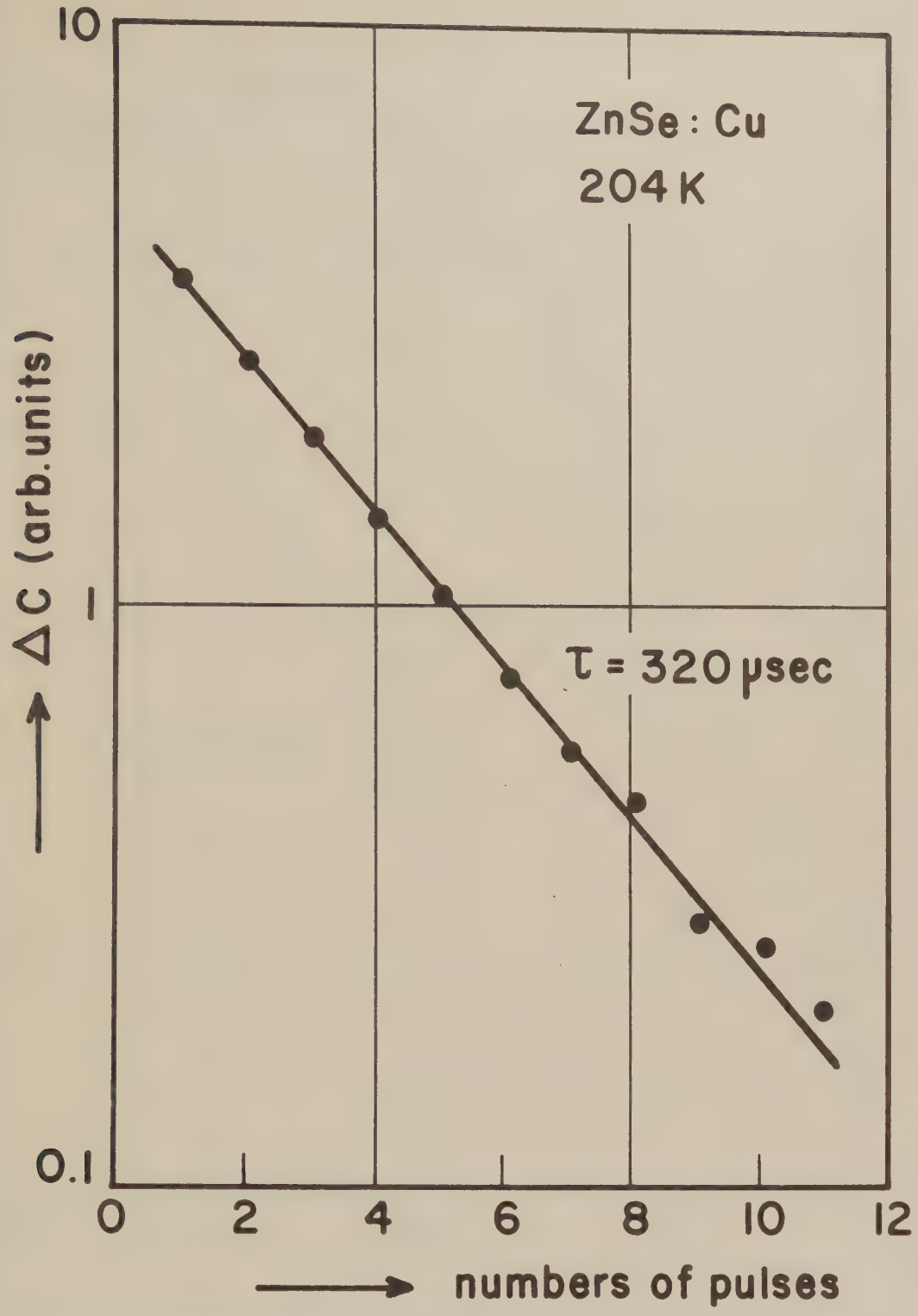

Capacitance change as a function of the number of voltage pulses applied to the diode. The length of these pulses was 100 μseconds.

Fig 12

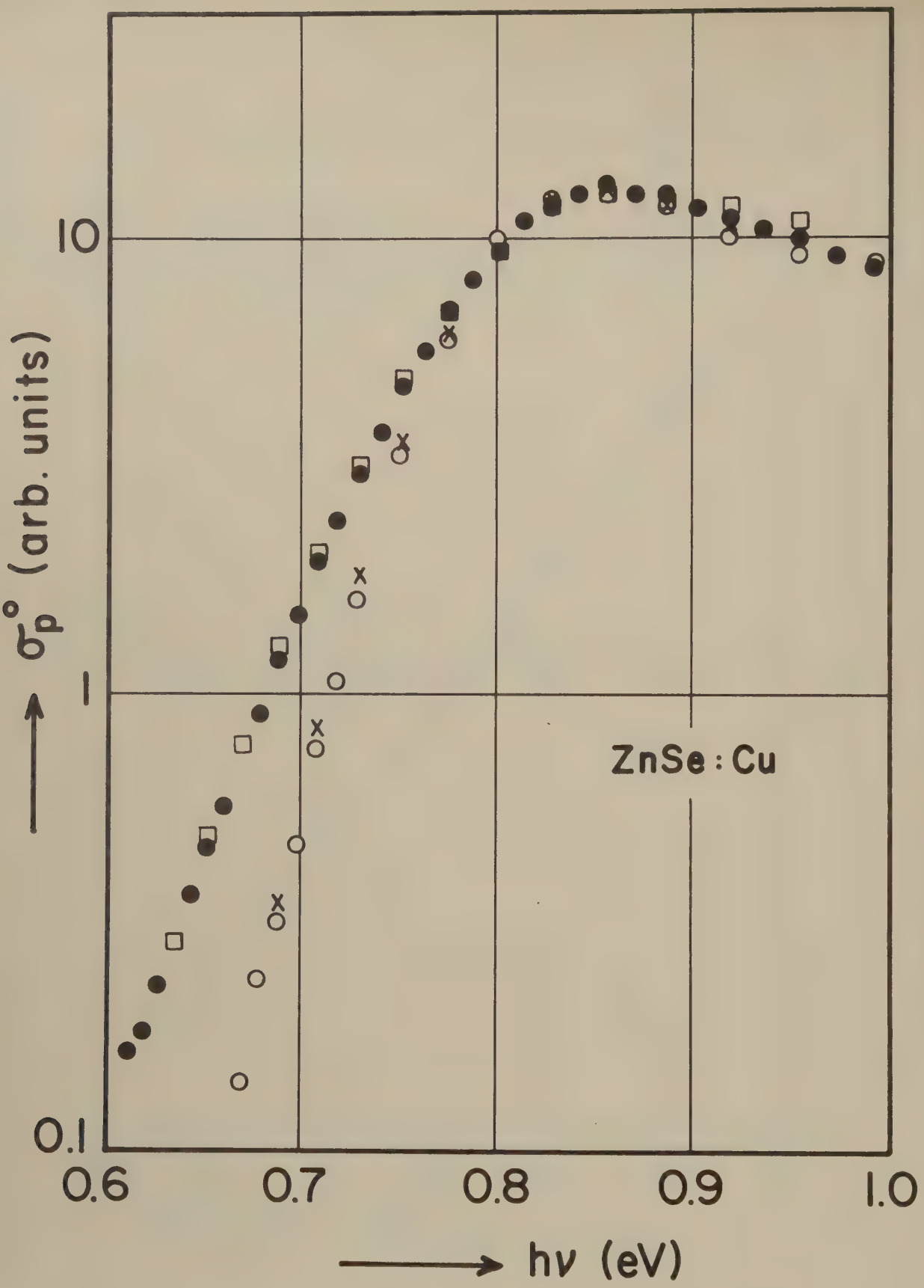

Spectra of the optical cross section σ_p^o obtained from the photocapacitance technique (● 205K, ○ 101K) and from the quenching of the photoconductivity (□ 205K, X 101K)

Fig 13

Fig 14

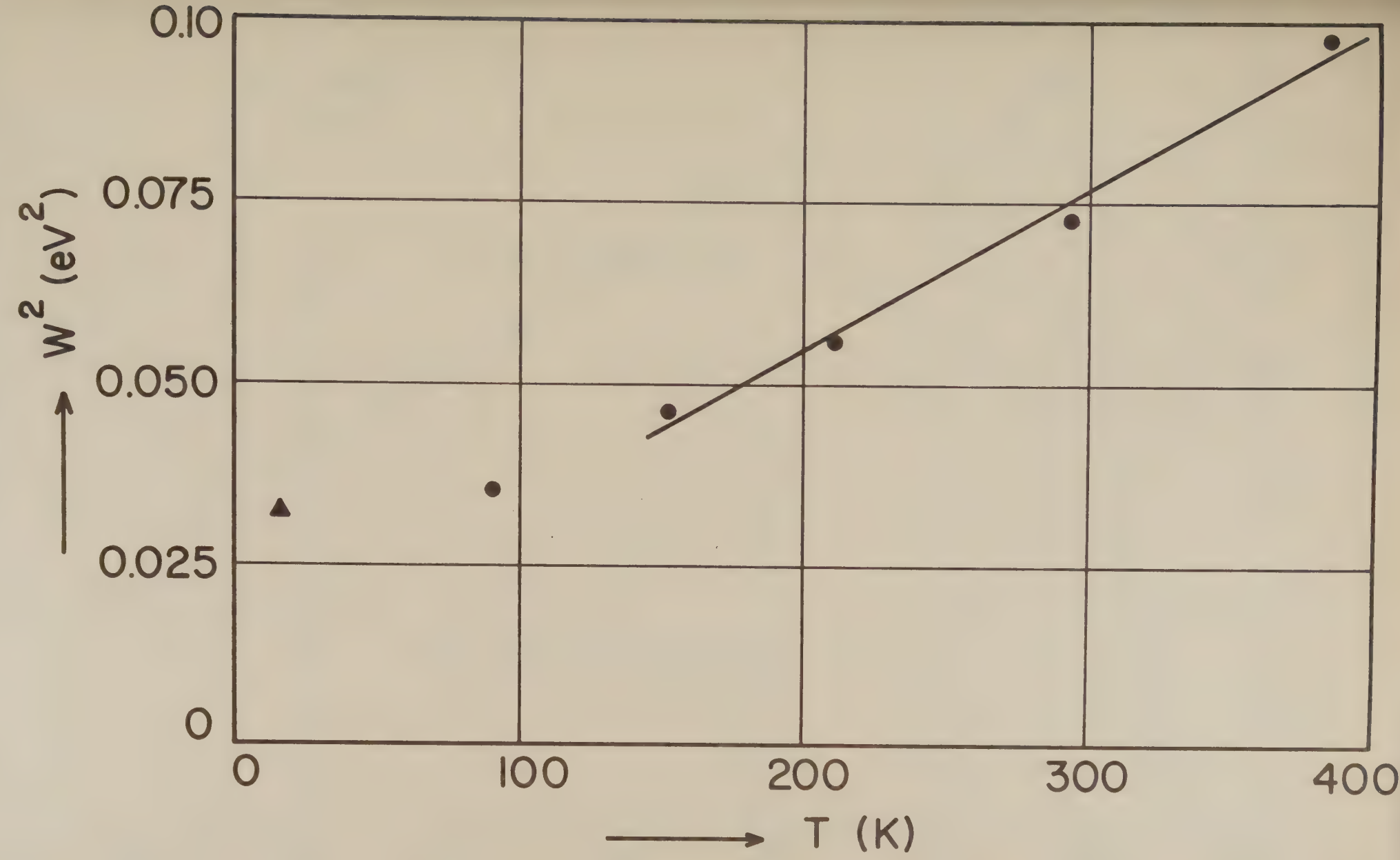

The square of the half-width of the red Cu emission as a function of temperature. The data are taken from reference 2 ●, and from reference 27 ▲.

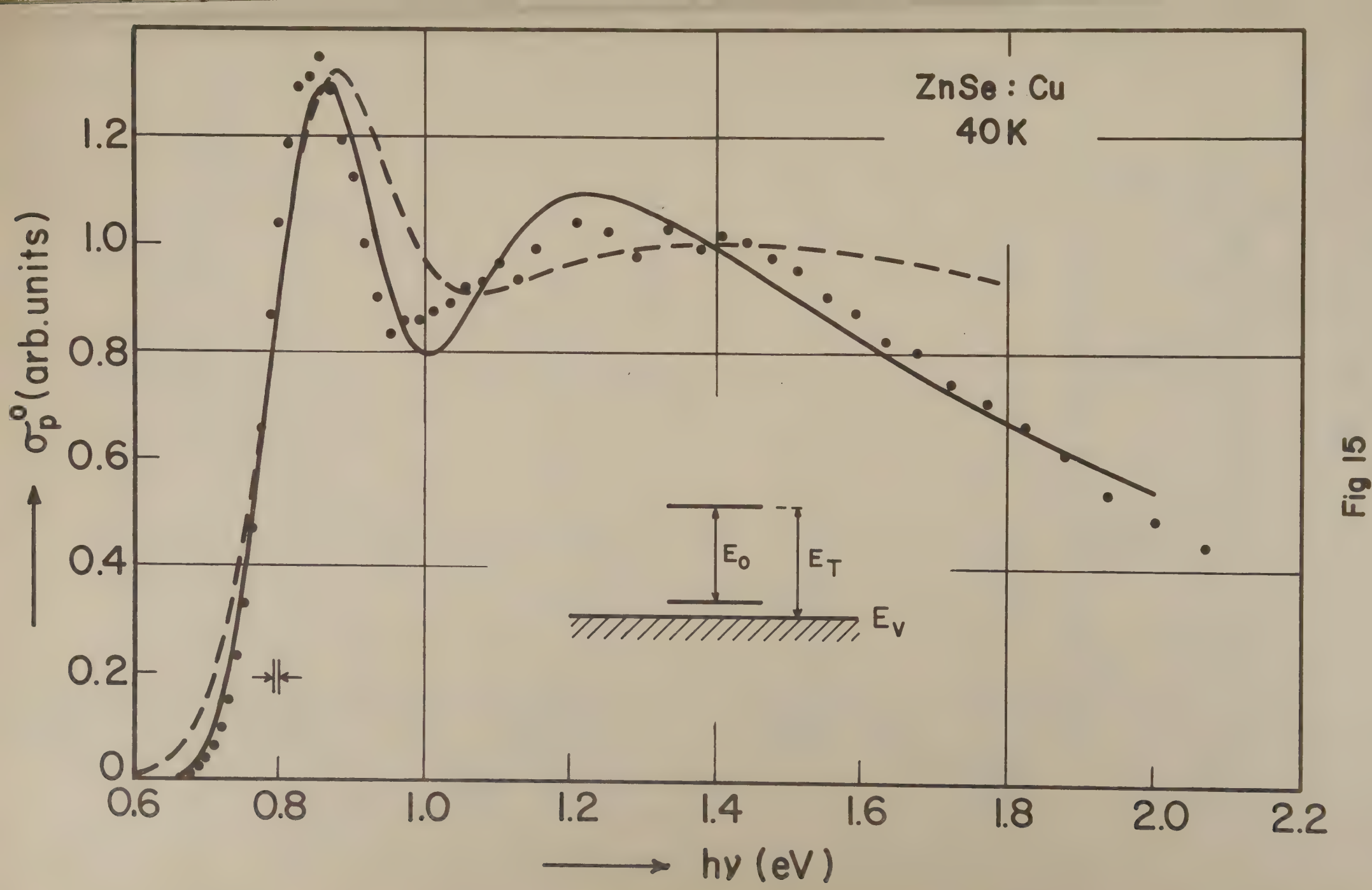
ZnSe : Cu
40K
σ_p^o (arb.units)
1.2
1.0
0.8
0.6
0.4
0.2
0
0.6
0.8
1.0
1.2
1.4
1.6
1.8
2.0
2.2
hν (eV)
E_o
E_T
E_v

Fig 15

Captions, figure 15 and 16.

FIGURE 15:
The spectrum of the optical cross section σ_p^o at 40K as obtained from the photocapacitance measurements and from calculations using equation 14 with $\lambda=9$ and $\hbar\omega=0.025$ eV. The energies E_T and E_o and the constants C_T and C_o are chosen to obtain the best fit to the experimental data.
Dots: Experimental data.
Solid line: σ_{el}^o according to equation 16 using $E_T=0.78$ eV, $E_o=0.65$ eV and $C_T/C_o=18$.
Dashed line: σ_{el}^o according to equation 17 using $E_T=0.48$ eV, $E_o=0.65$ eV and $C_T/C_o=32$.

FIGURE 16:
Spectra of the optical cross section σ_p^o at different temperatures as obtained from the photocapacitance measurements and from calculations using equations 14 and 16. The values of the constants used in the calculation are the same at all temperatures and are the values used obtaining the solid curve in figure 15.
Experimental data: ● 40K, X 101K, ○ 205K.
Calculated data: dotted line 40K, dashed line 101K, solid line 205K.

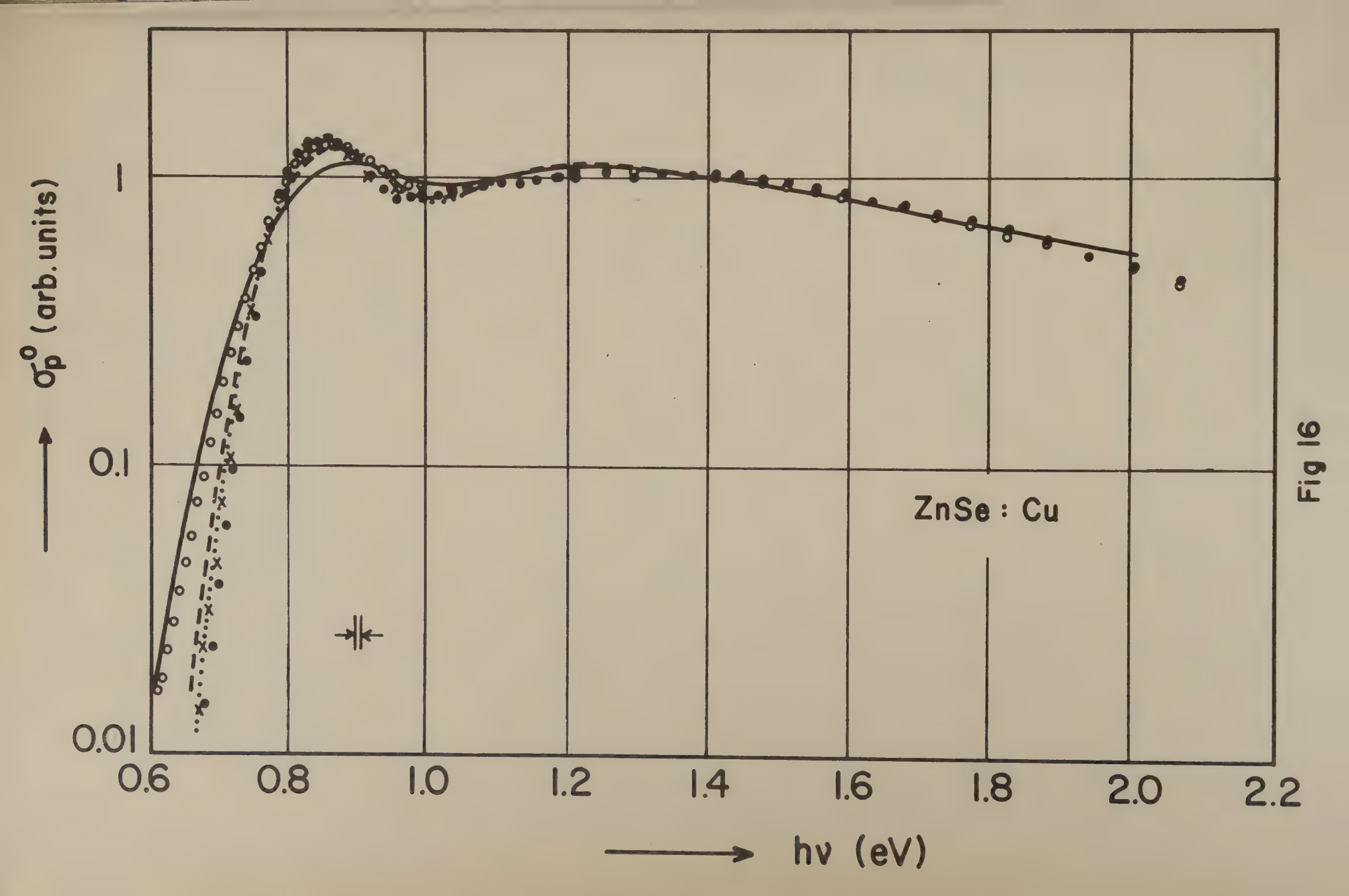

Fig 16

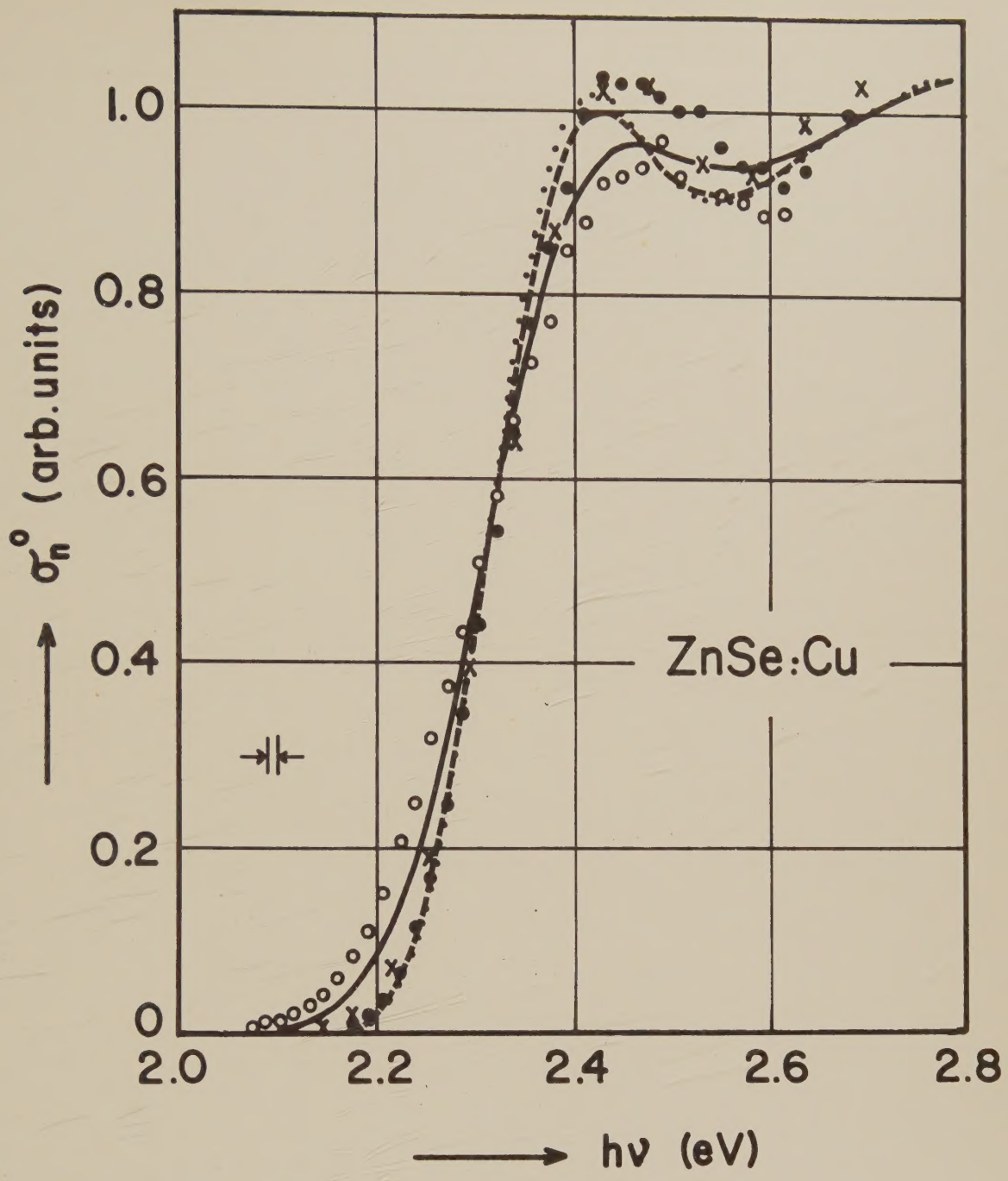

Spectra of the optical cross section σ_n^o at different temperatures as obtained from the photocapacitance measurements and from calculations using equations 14 and 16. The same values of the constants have been used at all temperatures. λ=9, $\hbar\omega$=0.025 eV, E_T=2.18 eV, E_o=2.17 eV and C_T/C_o=264.
Experimental data: ● 40K, ✕ 101K, o 205K.
Calculated data: dotted line 40K, dashed line 101K, solid line 205K.

Fig 17